SUPPORTING INFORMATION

Single-Cell Structural Lipidomics Using Miniature Dual-LIT Mass Spectrometer

Zhijun Cai, Ningxi Li, Simin Cheng, Zheng Ouyang, Xiaoxiao Ma*

TABLE OF CONTENTS

Experimental Procedures

Reagents and Materials. Tetraethylammonium bromide (TEAB), tetrabutylammonium bromide (TBAB), tatrahexylammonium bromide (THAB), tetraoctylammonium bromide (TOAB), tetrakis (decyl) ammonium bromide (TDAB) and tetra-n-dodecylammonium iodide (TDAI) and verapamil were purchased from J&K Scientific Ltd. (Beijing, China). Lipid standards were purchased from Avanti Polar Lipids (Alabama, USA). 2-acetylpyridine (2-AP) was purchased from Aladdin Biological Technology Company, Ltd. (Shanghai, China). Erastin was purchased from Macklin Inc. (Shanghai, China). Doxorubicin (DOX) was purchased from Jiangsu KeyGEN BioTECH Co., Ltd. (Nanjing, China). The low-pressure mercury lamp with UV emission centered around 254 nm (Model No. 80-1057-01) was purchased from BHK Inc. (Seongnam-SI, Korea). Dimethyl sulfoxide (DMSO), Dulbecco's modified Eagle medium (DMEM), phosphate-buffered saline (PBS) solution (10 mM, pH 7.4), Roswell Park Memorial Institute-1640 medium (RPMI), fetal bovine serum (FBS), and Dulbecco's phosphate-buffered saline (DPBS) were purchased from Gibco Life Technologies (Carlsbad, CA, USA). All other chemicals (HPLC-grade) were purchased from Fisher Scientific (NJ, USA) and used without further purification.

Sample preparation. MCF-7 cells were purchased from the National Infrastructure of Cell Line Resource (Beijing, China). BT-474 and MDA-MB-468 cells were obtained from Shanghai Enzyme Research Biotechnology Co. Ltd. (Shanghai, China). DOX-sensitive and DOX-resistant human chronic myelogenous leukemia (CML) K562 cells were purchased from Jiangsu KeyGEN BioTECH Co., Ltd. (Nanjing, China). MCF-7 and MDA-MB-468 were cultured in DMEM. BT-474, DOX-sensitive K562, and DOX-resistant K562 cells were cultured in RPMI. For ferroptosis, MDA-MB-468, BT-474, and MCF-7 cells were treated with 10nM Erastin for 24h, while the control group was treated with DMSO. All cells were supplemented with 10% FBS and 1% penicillin-streptomycin. For DOX-resistant K562 cells, 1μg/mL DOX in DPBS was additionally added. All cells were cultured in a breathable dish at 37 °C in a humidified atmosphere containing 5% CO_2. Cells were washed with DPBS (2 mL) and passaged by trypsinization when they reached 85−90% confluence.

After washing with PBS, cells (~10^6 cells/mL) were suspended in a methanol/H_2O mixture (1:1,

v/v) for 10 min in a shaker. They were then washed twice. For direct single-cell analysis, cells were diluted to 10^4 cells/mL.

A modified Folch method was used for lipid extraction from the cell population. Harvested cells were divided into two equal subsets. One subset was suspended in methanol/H_2O (1:1, v/v) while the other subset was treated with PBS as a control. After centrifugation, cells were resuspended in 1 mL deionized water in a 10 mL centrifuge tube, followed by the addition of 1 mL methanol and 2 mL chloroform. The internal standard (PC 30:0 and PE 34:0) was added at a concentration of 5 μM. After 5 min vortexing, the mixture was centrifuged at 11,269g for 8 min. Then, a second round of lipid extraction was performed. The chloroform layers from the two extractions were finally combined and dried under a nitrogen flow. The lipid extract was reconstituted in 500 μL methanol/acetonitrile (1:1, v/v) and stored at −20 °C for mass spectrometry (MS) analysis.

The stainless-steel electrode (o.d. = 120 μm) was purchased from HAMILTON Company (Reno, NV, USA), and the borosilicate glass capillaries (i.d. = 0.86 mm, o.d. = 1.5 mm) were purchased from Sutter Instrument (Novato, CA, USA). Borosilicate glass capillaries were washed with 1% formic acid (v/v) in ethanol/water (1:1, v/v) twice and then pulled to make nanoESI emitters (i.d. of the opening ≈ 5~10 μm) for MS analysis, using a P-1000 micropipette puller (Sutter Instrument, Novato, CA, USA). P-1000 parameters are as follows: HEAT = 535, PULL = 0, VEL = 15, DELAY = 1, Pressure = 600, and Ramp = 530.

Single-cell MS analysis. Around 0.5 μL of cell suspension (10^4 cells/mL) was transferred to a nanoESI capillary. Then, the cells were migrated to the tip by gravity (Supplementary Figure 1a). A microscope was used to determine if there was only a single cell at the capillary tip. A video of the cell migration is available in the appendix. To enable the identification of lipid fine structure, lipid derivatization based on PB (Paternò-Büchi) reaction was necessary.[1] This step is described in detail in the "Online PB reaction for single cells" section of "Results and Discussion". Finally, a droplet (~50 μL) of methanol/ acetonitrile (1:1, v/v) with 1% formic acid was applied to the capillary tip, and a voltage of +1.8 kV was applied to initiate on-demand MS analysis. Unless otherwise specified, all MS analyses were conducted using a homebuilt miniature dual-LIT (linear ion trap) mass spectrometer system.

Dual-LIT MS System. The miniature dual-LIT MS system had the dual-LIT to perform collision-induced dissociation (CID) and mass analysis. Mass analysis used a scan rate of 1666.7 Da/s to acquire MS spectra. The miniature dual-LIT MS system had the DAPI (discontinuous atmospheric pressure interface). Since the ion introduction of DAPI was discontinuous, the opening time of the DAPI and ion source was synchronized. Due to the short time needed for the auxiliary electrospray, it was necessary to match the electrospray voltage and the DAPI opening time. The miniature MS system with the DAPI adopted a discontinuous injection mode. In a single analysis, high voltage was applied, and DAPI was turned on after a fixed delay. The peak intensity of *m/z* 760 was used as the reference peak to optimize the opening time difference between the ion source and DAPI (Supplementary Figure 4a).

The miniature MS system with the DAPI has added a new vacuum pressure regulation system, which can ensure the stability of vacuum pressure during different ion operations. The original miniature MS system used air at atmospheric pressure to regulate vacuum pressure, which could not achieve long-term stable regulation of pressure, which brought challenges to multiple serial analyses. The developed vacuum pressure regulation system used the air between the diaphragm pump and turbo pump (Supplementary Figure 5a) and could achieve multi-channel stable pressure regulation.[2] With the vacuum pressure regulation system, the miniature dual-LIT MS could be capable of long-time ion storage (up to ~30 s) in LIT with only 5-10% ion loss (Supplementary Figure 5b-5c). MSAT (Mass Selective Axial Transfer) and CID processes required higher vacuum pressure, and their optimal pressure range was 10^{-3}~10^{-2} Torr. The mass analysis process required lower vacuum pressure; its optimal pressure range was 10^{-3}~10^{-4} Torr. At the same time, keeping the vacuum pressure in the vacuum chamber greater than 10^{-4} Torr was conducive to the long-term retention of ions in LIT 1.

For a single injection, the DAPI opening time was 20 ms, the pressure cooling time was 80 ms, and the total was 100 ms. For subsequent operations, including MSAT, CID analysis, and mass analysis, the work time was 900 ms. For example, the total time for 27 MS/MS analyses was about 25 seconds (Supplementary Figure 6).

Nomenclature. *n*-nomenclature was employed for C=C location notations in this work. For example, PC 18:0/18:1 (*n*-9) denotes that a monounsaturated 18-carbon fatty acyl chain is at the *sn*-2 position, and one double-bonds at the 9th C-atom counted from the aliphatic end of hydrocarbon residue. The "0" and "1" following the carbon number represent the degree of unsaturation of the fatty acyl chain. When the *sn*-position of the fatty acid chain was not determined, it was indicated by '_', such as PC 18:0_18:1.

Data processing. The peak heights of the corresponding lipid sum composition, C=C, and *sn*-isomers diagnostic ions of the target lipid species were extracted and analyzed throughout this study for quantitation. When performing statistical analyses of different lipid isomers, all isomer-specific ions were used to represent the amount of a specific isomer. Data processing, including distribution fitting, *t*-test, *t*-SNE calculation, and *k*-means clustering, was performed using MATLAB 2019a (MathWorks Inc.). Hierarchical cluster analysis was performed using MetaboAnalyst with default software parameters (https://www.metaboanalyst.ca/MetaboAnalyst/ModuleView.xhtml).[3]

Results and Discussion

Multiple Mass-selective Partial Transfer. MMPT (Multiple Mass-selective Partial Transfer) was proposed compared to MSAT (Mass Selective Axial Transfer). As shown in Supplementary Figure 6, the target ions with the specific *m/z* could be transferred in three equal ratios by MMPT. Compared with MSAT, the energy of the auxiliary AC was reduced. Within a particular range, the ion single transmission ratio was linearly correlated with the amplitude of the auxiliary AC (Supplementary Figure 7). With multiple partial transfers, ion losses would occur. The experiment was compared with 1 part (single rate 100%), 2 parts (single rate 50%), 3 parts (single rate 30%), 5 parts (single rate 20%) and 10 parts (single rate 10%) of equal proportional transfer. No significant ion loss occurred under the first three conditions (Supplementary Figure 8a-f). Considerable loss of ions occurs when the number of partial transmissions is no less than 5 times (Supplementary Figure 8g-l). This may be the result of the accumulation of multiple losses. We performed no more than three partial transmissions in experiments to avoid this phenomenon.

Theoretical model and simulation method. The radius of the LIT rod is r_0, of 4mm. The ions were trapped by an electric potential $\emptyset$, containing a direct current (DC) component, U, and a radio frequency (RF), V_{RF}, component driven by a dual-phase RF at a frequency, Ω, of $2\pi \times 1\ MHz$. This yields:

$$\emptyset = \left(\frac{x^2 - y^2}{r_0^2}\right)\left(U - V_{RF}cos\Omega t\right) \qquad (1)$$

The interaction of the ions could be described by an effective space charge filed, E_{SC}, which yields

$$E_{SCu}(\vec{r}) = \frac{eNu}{2\pi r^2 \epsilon_0 z_0}\left\{1 - \exp\left[-\frac{\left(\vec{r} - \vec{r}_c\right)^2}{2\sigma_u^2}\right]\right\}(u = x,y) \quad (2)$$

Which e was electron charge, ϵ_0 is the vacuum permittivity, u denotes the x or y direction, N is the ion Number, $\vec{r}$ is the spatial coordinate, and $\vec{r}_c$ and σ_u are the mean and distribution width of the ions, respectively. The equation of ion motion in the RF field with ion interactions is as follows

$$m\ddot{u} = -e\nabla_u\emptyset + e\sum_i E_{SCu}^{\ i} \qquad (3)$$

Where m and e are mass and electron charge of the ion, respectively. i denotes the ion clouds of different species. In eq 3, the DC and RF components of $\emptyset$ could be characterized by Mathieu parameters, a_u and q_u

$$a_x = -a_y = \frac{8eU}{m\Omega^2 r_0^2};\ q_x = -q_y = \frac{4eV_{RF}}{m\Omega^2 r_0^2} \qquad (4)$$

For LIT, U is set to 0 and attention should be paid to q (q_x) value. When q<0.908, ions are stable in the LIT. Applying auxiliary AC can excite stable ions, whose frequency is determined by the q value.

The ions are initially placed in the LIT center with a spatial distribution σ_u of $0.02 r_0$ at an ion temperature T_{ion} of 300K. Then they collided with background molecules at a pressure of $1 \times 10^{-5}\ Torr$. The ion trajectories were calculated using a homemade simulation program. Briefly, the program simulated ion trajectory through the calculation of two successive processes in each step: the ion trajectory is calculated within a collision-free path in a pure electric field and then in an ion-neutral collision, modifying the ion velocity and the ion trajectory. The effective electric field due to the collective interaction of ions was modeled using eq 2. The collision-free path was generated according to the mean free path of the ions, and the ion-neutral collisions were modeled using a stochastic Monte Carlo hard-sphere model. When the ion number N > 1000, a rapid simulation algorithm is applied.[4]

Online PB reaction for single cells. Following cell migration and solvent evaporation, a droplet (~50 μL) of assistant derivatization solvent (acetonitrile: water = 1/1 (v/v) with 10 mM 2-AP) was applied to the capillary tip. After 30 seconds of UV irradiation for the PB reaction[1] (Supplementary Figure 12), the solvent evaporated. Subsequently, a droplet (~50 μL) of methanol/acetonitrile (1:1, v/v) with 1% formic acid was applied to the capillary tip for on-demand nanoESI. For *sn*-position analysis, a droplet of 100 μM sodium acetate in methanol/acetonitrile (1:1, v/v) was used as the assistant solvent.

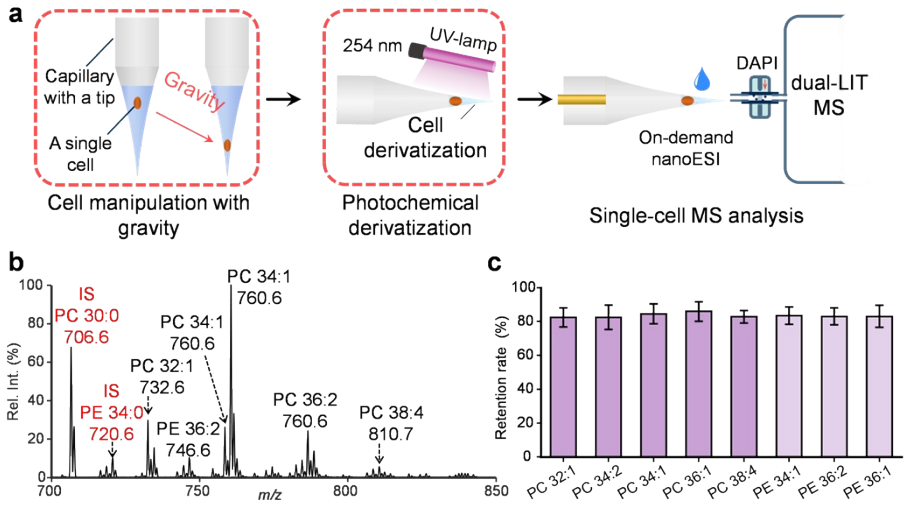

Supplementary Figure 1. Single-cell MS. (a) The flow chart of single-cell MS using dual-LIT MS platform: migration of single cells in the capillary using gravity; photochemical derivatization of lipids from a single cell; and ionization of lipids from a single cell. (b-c) Evaluation of lipid retention efficiency after cell fixation. These analyses were performed by LTQ XL mass spectrometer (Thermo Scientific, San Jose, CA). (b) An MS1 spectrum of fixed cell extracts with internal standards (IS). (c) The retention rate of typical lipids (repeated 5 times), and error bars represent standard deviations (SDs).

$$Retention\ Rate_{PC} = \frac{I(184)^{after\ fixation}_{PC} \cdot I(184)^{before\ fixation}_{PC\ 30:0}}{I(184)^{before\ fixation}_{PC} \cdot I(184)^{after\ fixation}_{PC\ 30:0}},$$

$$Rentention\ Rate_{PE} = \frac{I(Precursor - 141)^{after\ fixation}_{PE} \cdot I(579)^{before\ fixation}_{PE\ 34:0}}{I(Precursor - 141)^{before\ fixation}_{PE} \cdot I(579)^{after\ fixation}_{PE\ 34:0}}.$$

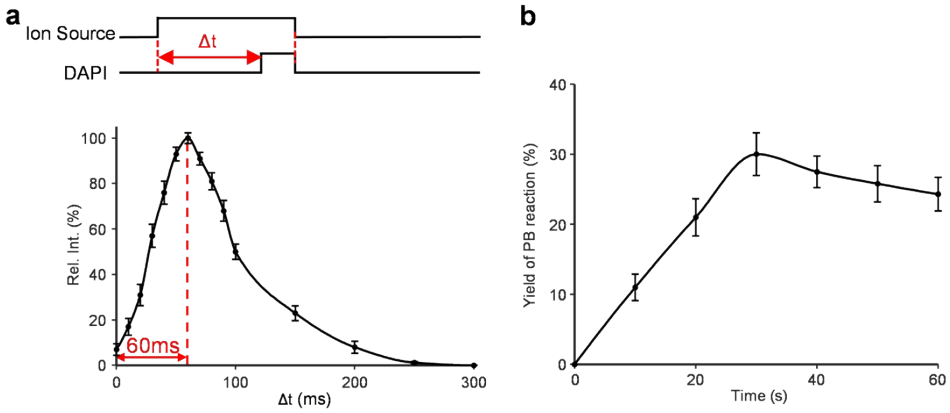

Supplementary Figure 2. Optimization using MDA-MB-468 cell extracts. (a) Timing matching of the ion source and discontinuous atmospheric pressure interface (DAPI). Droplets (~10 μL) of cell extract

in methanol/acetonitrile (1:1, v/v) with 1% formic acid were applied to the capillary tips for the optimization. The peak intensity of *m/z* 760 was used as the reference. (b) Relationship between reaction time and yield. For optimization of PB reaction time, 0.5 μL of cell extracts in acetonitrile/water (1:1, v/v) with 10 mM 2-AP was transferred to the nanoESI capillary. $Yield = \frac{\sum Int.\,(^{PB}(Precusors))}{\sum Int.\,(^{PB}(Precusors)) + \sum Int.(remaining\ Precurosrs)}$. Error bars represent SDs (N=5).

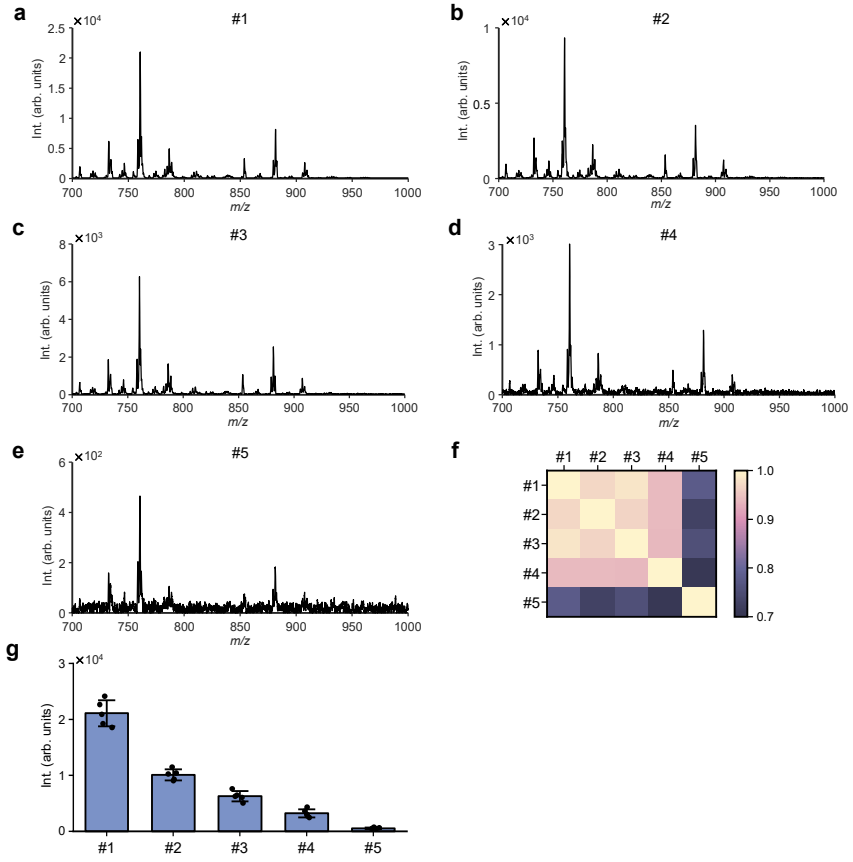

Supplementary Figure 3. MS spectra for the single MDA-MB-468 cell. (a) #1 injection, (b) #2 injection, (c) #3 injection, (d) #4 injection and (e) #5 injection. (f) Pairwise correlation coefficients were calculated using the intensities of PB product ions of each spray. g) Intensities of *m/z* 760 for 5 injections (N=5). Error bars represent SDs.

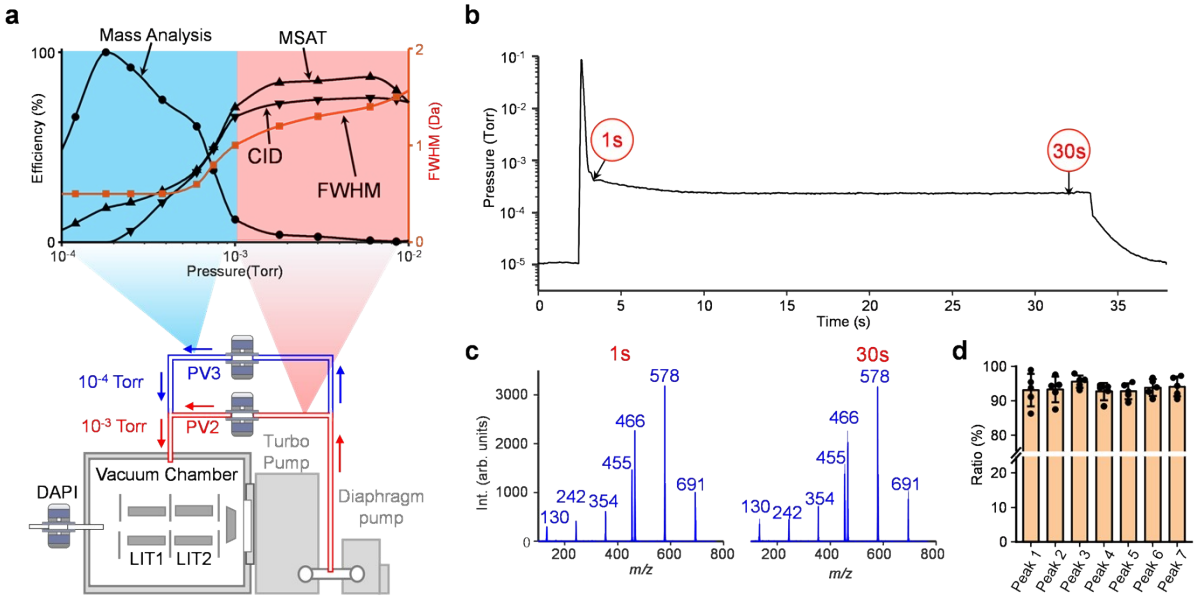

Supplementary Figure 4. Vacuum adjustment system of the dual-LIT mass spectrometer. (a) The system utilizes the gas between the turbo pump and the diaphragm pump to assist in vacuum adjustment of the vacuum chamber. The regulation system consists of two vacuum regulation lines, of which the blue part regulates the pressure in the range of 10^{-4}~10^{-3} Torr, which is beneficial for mass analysis. The red part regulates the pressure in the range of 10^{-3}~10^{-2} Torr, which is beneficial for CID and MSAT processes. Optimization curves were obtained by analyzing verapamil in methanol (*m/z* 455, 1μg/mL). Mass analysis and CID are performed in the LIT 2. $Efficiency_{Mass\ Analysis} = \frac{I(455)}{Max\{I(455)\}}$, $Efficiency_{MSAT} = \frac{I(455)_{MSAT}}{I(455)_{Transfer\ directly}}$, $Efficiency_{CID} = \frac{I(165)+I(303)}{I(455)_{raw}-I(455)_{remaini}}$

FWHM: Full width at half maxima. (b-d) Pressure curve when the PV3 valve is open for a long time. (c) MS spectra of ions stored in LIT 1 for different time, including 1s and 30s. (d) Storage efficiency of the seven types of ions in 5 replicates. Peak 1: *m/z* 130; Peak 2: *m/z* 242; Peak 3: *m/z* 354; Peak 4: *m/z* 455; Peak 5: *m/z* 466; Peak 6: *m/z* 578; Peak 7: *m/z* 691; $Ratio = \frac{I(Peak\ N)_{30s}}{Average\ [I(Peak\ N)_{1s}]}, N = 1-7.$ Error bars represent SDs.

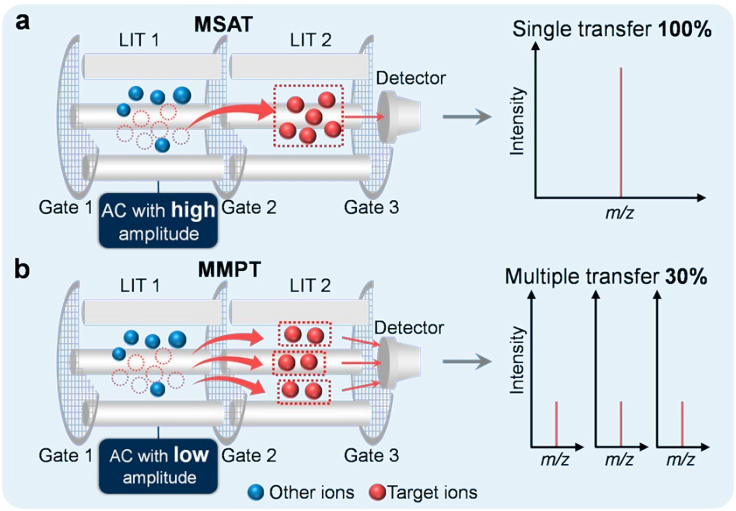

Supplementary Figure 5. Comparison of MSAT and MMPT. (a) An AC signal with a higher amplitude was applied for MSAT to selectively transfer all ions of a specific *m/z* in a single transfer process. There was ion loss in the MSAT process, and the maximum transmission efficiency was defined as 100%. (b) An AC signal with a lower amplitude was applied for MMPT to selectively transfer a certain ratio of a specific *m/z* ions multiple times. The transmission efficiency there referred to the maximum transmission efficiency of MSAT.

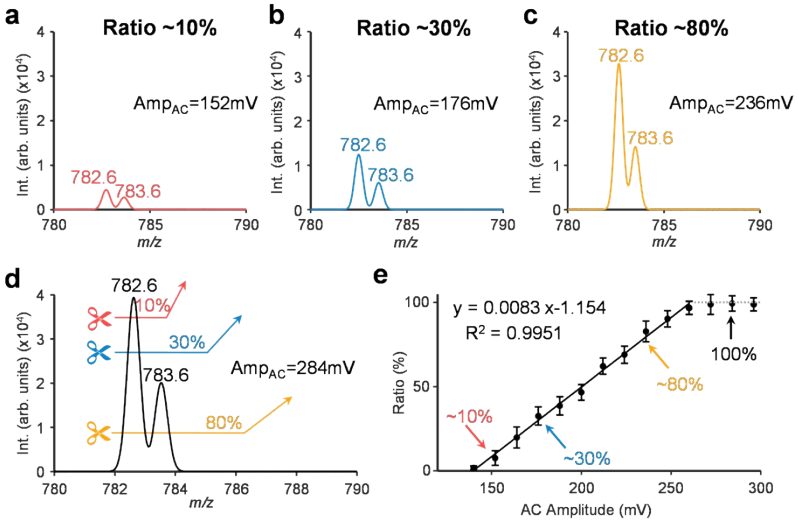

Supplementary Figure 6. Different transfer ratios with different AC amplitude for the ion [PC 34:1+Na]$^+$ (*m/z* 782.6). 10 μM PC 34:1+100μM sodium acetate in acetonitrile/water (1:1, v/v). (a) Ratio ~10% with AC amplitude 152mV, (b) ratio ~30% with AC amplitude 176mV, (c) ratio ~80% with AC amplitude 236mV, (d) ratio 100% with AC amplitude 284mV. (e) Relationship between

transfer ratio and AC amplitude. The transmission efficiency of the last four points was 100% (gray dotted line), which was the MSAT process. Error bars represent SDs (N=5).

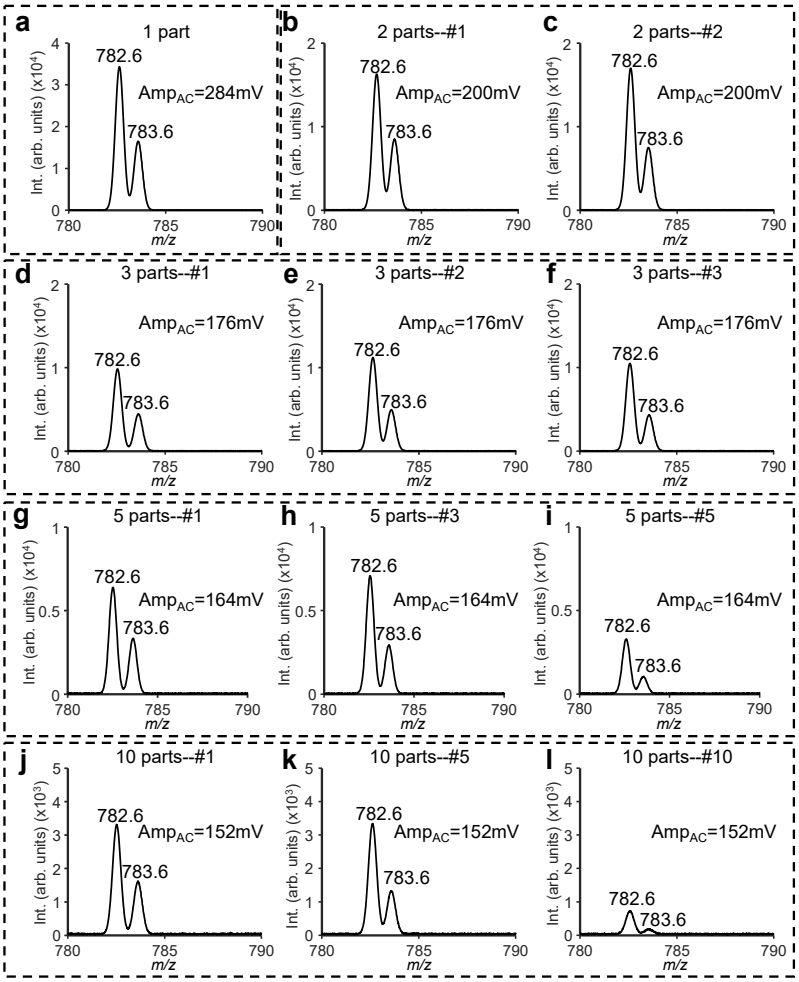

Supplementary Figure 7. MMPT for ion $[PC\ 34:1+Na]^+$ (*m/z* 782.6). 10 µM PC 34:1+100µM sodium acetate in methanol/acetonitrile (1:1, v/v)). (a) MS1 spectrum of MSAT with AC amplitude 284 mV. (b-c) MS1 spectra of MMPT for 2 parts with AC amplitude 200 mV. MS1 spectrum of (b) #1 part and (c) #2 part. (d-f) MS1 spectra of MMSPAT for three parts with AC amplitude 176 mV. MS1 spectrum of (d) #1 part, (e) #2 part, and (f) #3 part. (g-i) MS1 spectra of MMPT for five parts with AC amplitude 164 mV. MS1 spectrum of (g) #1 part, (h) #3 part, and (i) #5 part. (j-l) MS1 spectra of MMPT for 10 parts with AC amplitude 152 mV. MS1 spectrum of (j) #1 part, (k) #5 part, and (l) #10 part. Average of 5 replicates.

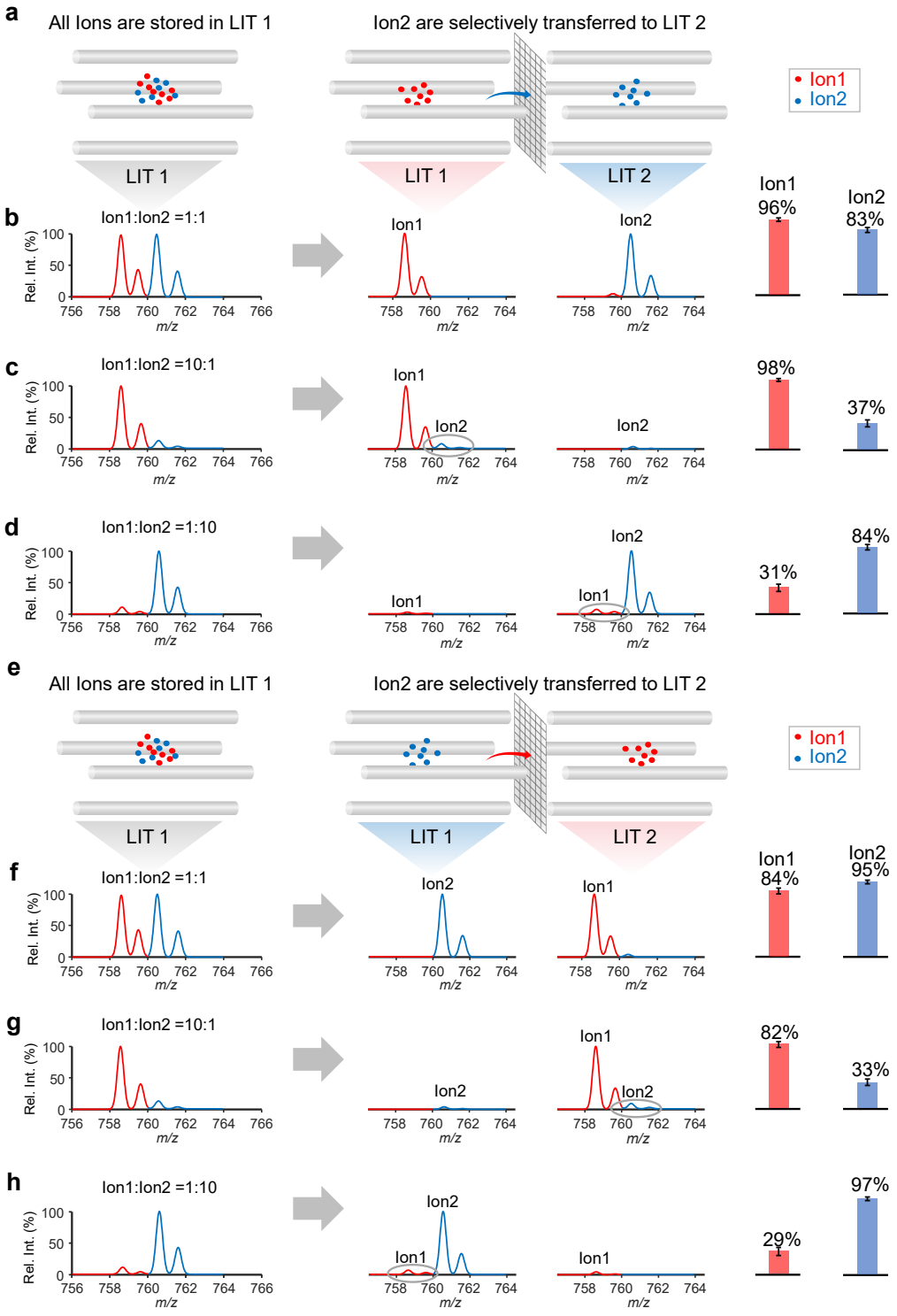

Supplementary Figure 8. The phenomenon of mutual interference between ions during the MSAT. Ion1 ([PC 34:2+H]$^+$, *m/z* 758.6), Ion2 ([PC 34:1+H]$^+$, *m/z* 760.6). By default, the peak intensity was proportional to the number of ions. For mass analysis, ions were scanned from LIT 1, and LIT 2 was an ion guide. When the ions were in LIT 2, ions were directly scanned from LIT 2. (a-d) There was a change in the number of ions when Ion1 was retained in LIT 1, and Ion2 was selectively transferred to LIT 2. (a) Schematic diagram of the process. (b) Ion1:Ion2 = 1:1, (c) Ion1:Ion2 = 10:1, and (d)

Ion1:Ion2 = 1:10. (e-h) There was a change in the number of ions when Ion2 was retained in LIT 1, and Ion1 was selectively transferred to LIT 2. (e) Schematic diagram of the process: (f) Ion1:Ion2 = 1:1, (g) Ion1:Ion2 = 10:1, and (h) Ion1:Ion2 = 1:10. The reference standard was the peak intensity of the MS1 spectrum obtained by directly scanning the two ions from LIT1 without any selection. These experiments were conducted in five replicates. Error bars represent SDs (N=5).

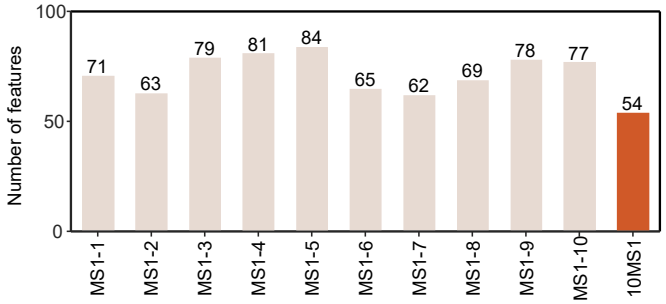

Supplementary Figure 9. Number of mass spectral features (MS1-1, …, MS1-10) and number of stable mass spectral features (10 MS1) after 10 single-cell MS1 analyses.

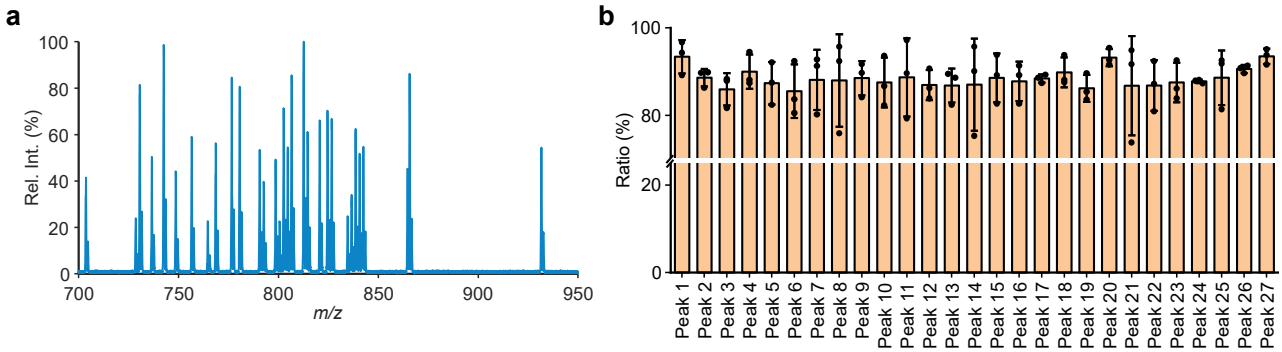

Supplementary Figure 10. (a) Low-abundance ions left in the LIT 1 after applying the SWIFT wave. (b) Isolation efficiency of 27 low-abundance ions in 3 replicates. Error bars represent SDs.

$$Ratio = \frac{I(Peak\ N)_{after\ SWIFT}}{Average\ [I(Peak\ N)_{before\ SWIFT}]},\ N = 1 - 27.$$

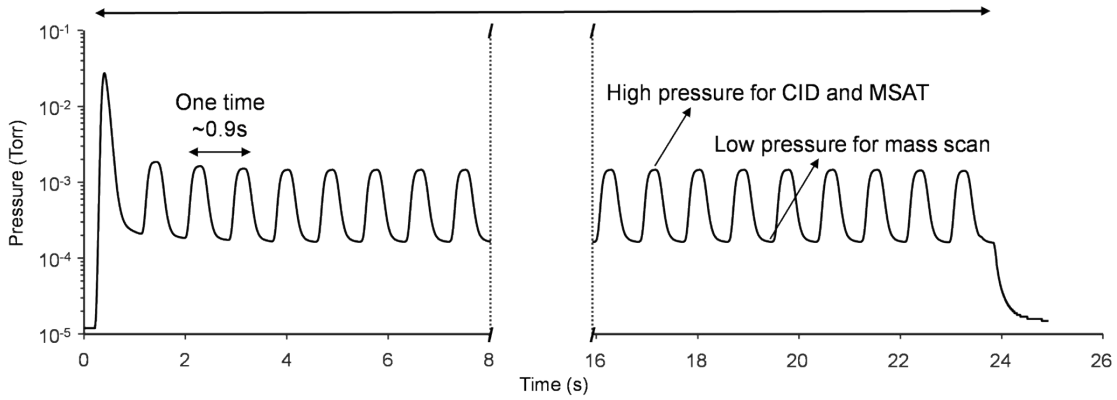

Supplementary Figure 11. Pressure curve for 27 times MS/MS analysis.

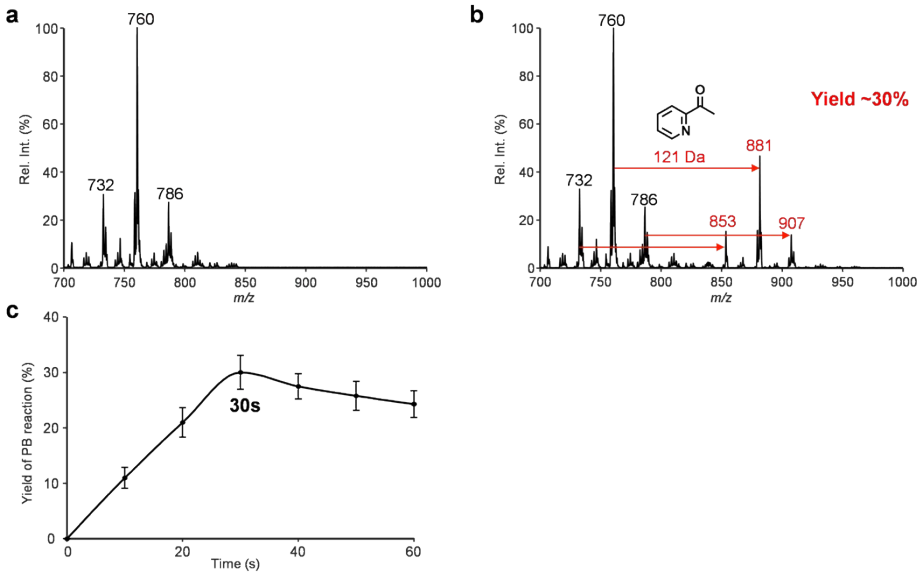

Supplementary Figure 12. The MS spectra of single MDA-MB-468 cells before and after PB reaction based on the dual-LIT MS platform. The MS spectra (a) before PB reaction, and (b) after PB reaction. $Yield = \frac{\sum Int.\,(^{PB}(Precusors))}{\sum Int.\,(^{PB}(Precusors)) + \sum Int.(remaining\ Precurosrs)}$. (c) Relationship curve between PB reaction efficiency and reaction time, and error bars represent SDs (N=5).

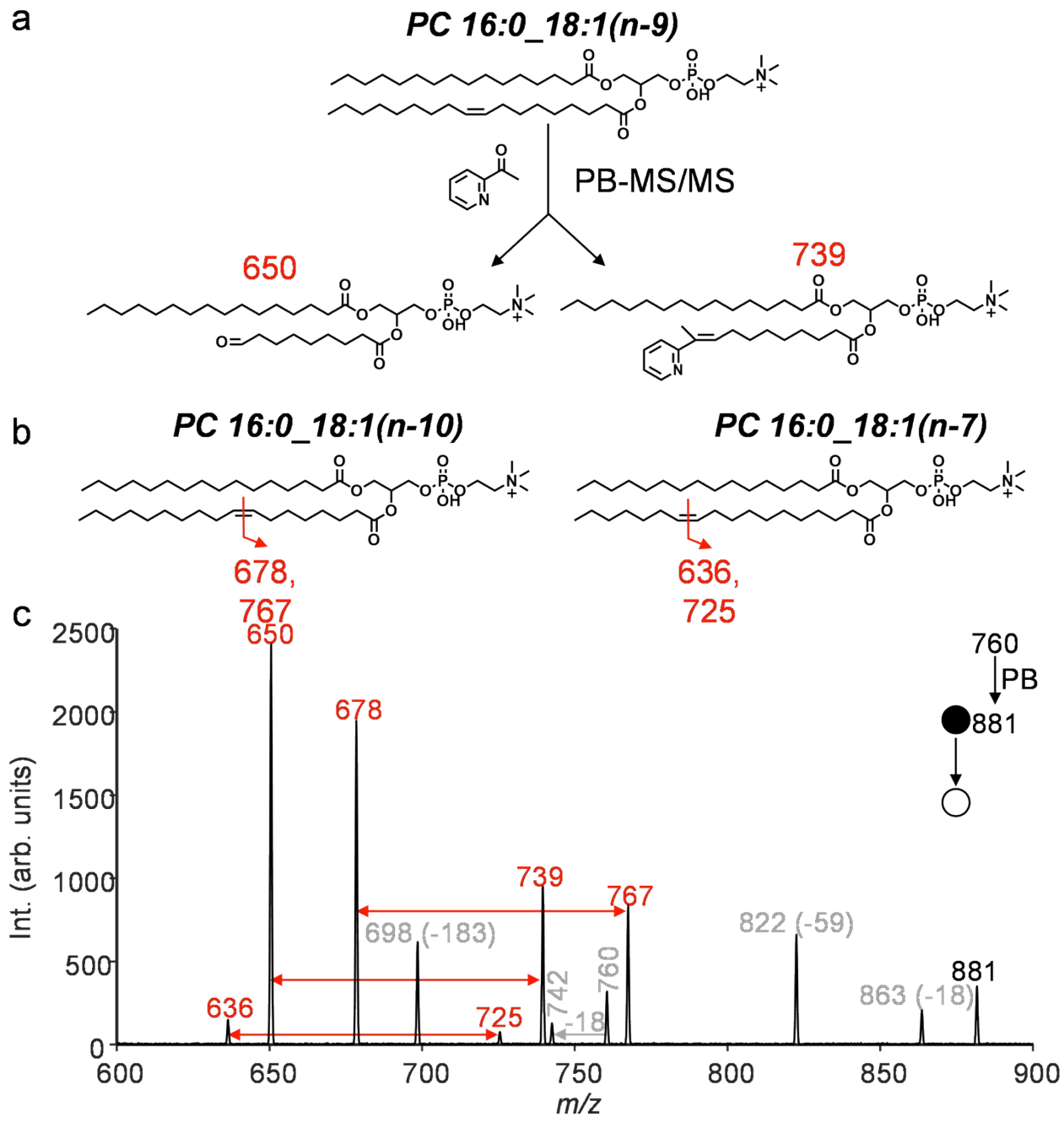

Supplementary Figure 13. (a) Structure of PC 16:0_18:1(*n*-9) and diagnostic fragments of C=C location after PB-MS/MS. (b) Structure of PC 16:0_18:1(*n*-10) and 16:0_18:1(*n*-7), and their diagnostic fragments of C=C location after PB-MS/MS. (c) MS/MS of $[^{PB}$ PC 34:1+H$]^+$ of a single MDA-MB-468 cell.

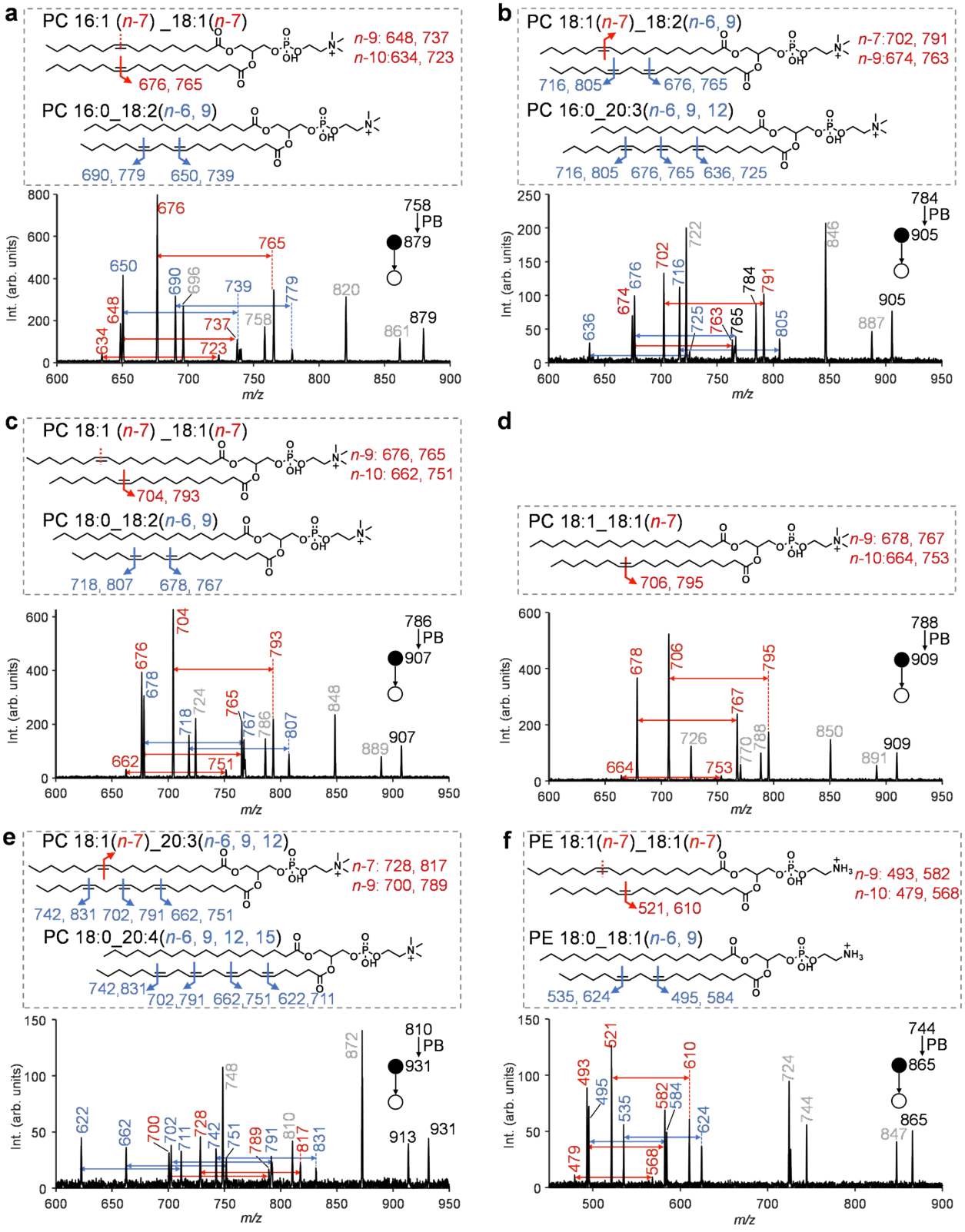

Supplementary Figure 14. MS/MS spectra after PB reaction of a single MDA-MB-468 cell. (a) MS/MS of [^{PB} PC 34:2+H]$^+$. (b) MS/MS of [^{PB} PC 36:3+H]$^+$. (c) MS/MS of [^{PB} PC 36:2+H]$^+$. (d) MS/MS of [^{PB} PC 36:1+H]$^+$. (e) MS/MS of [^{PB} PC 38:4+H]$^+$. (f) MS/MS of [^{PB} PE 36:2+H]$^+$.

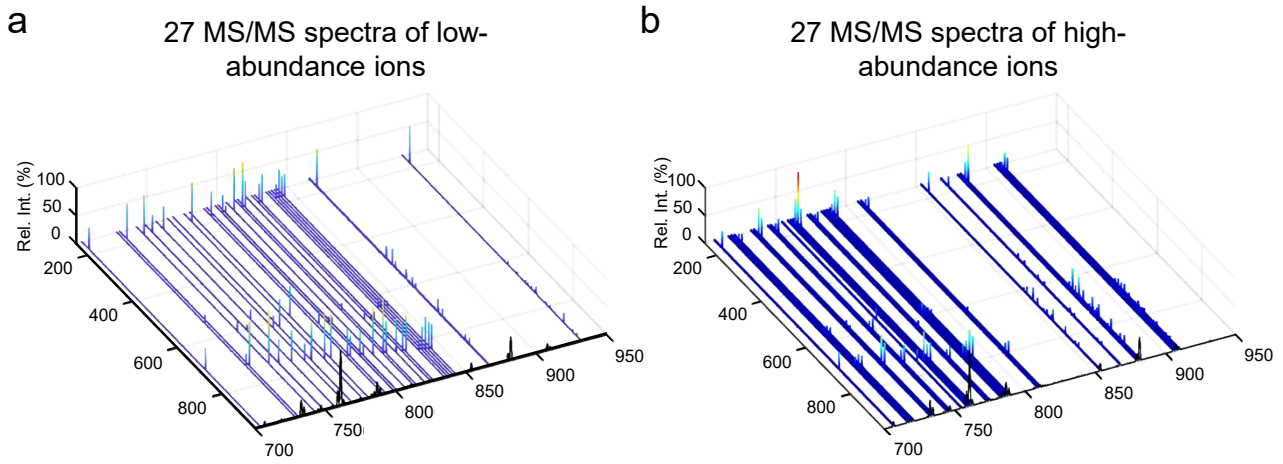

Supplementary Figure 15. Multiple MS/MS of a single MDA-MB-468 cell. (a) 27 MS/MS spectra of low-abundance ions (normalized to the max peak intensity of 27 MS/MS spectra), (b) 27 MS/MS spectra of high-abundance ions (normalized to the max peak intensity of 27 MS/MS spectra).

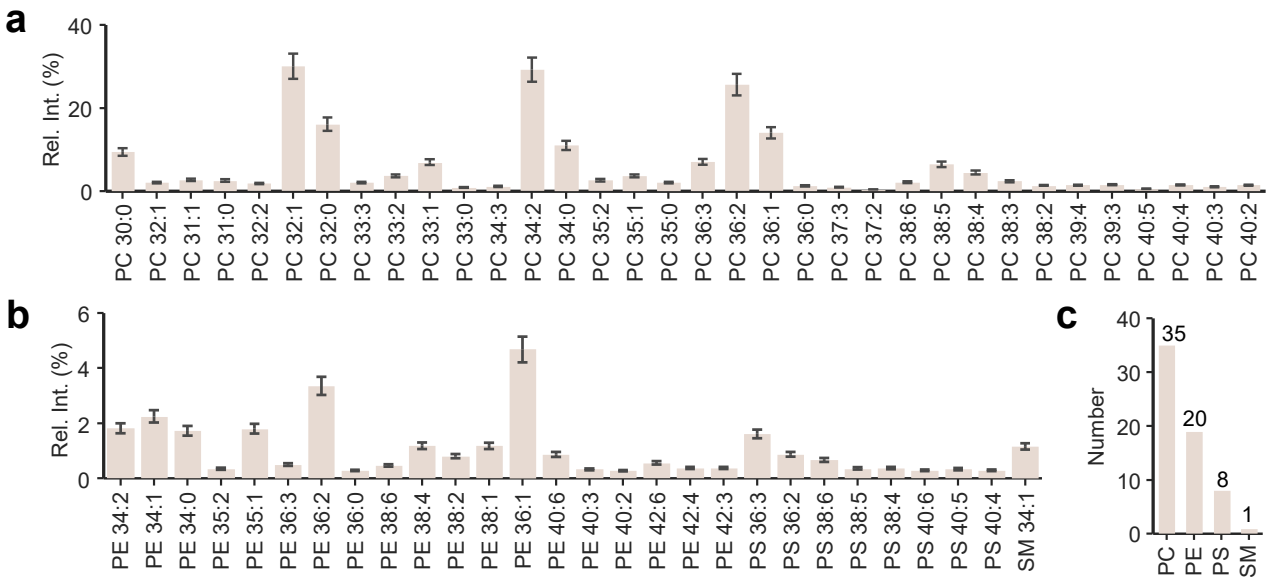

Supplementary Figure 16. The relative intensity (Rel. Int. (%)) of lipid sum compositions identified from single MDA-MB-468 cells (normalized to the intensity of fragment *m/z* 184 of PC 34:1). (a) PCs. (b). PEs, PSs, and SM. Error bars represent SDs (N=10). (c) Total number for lipids.

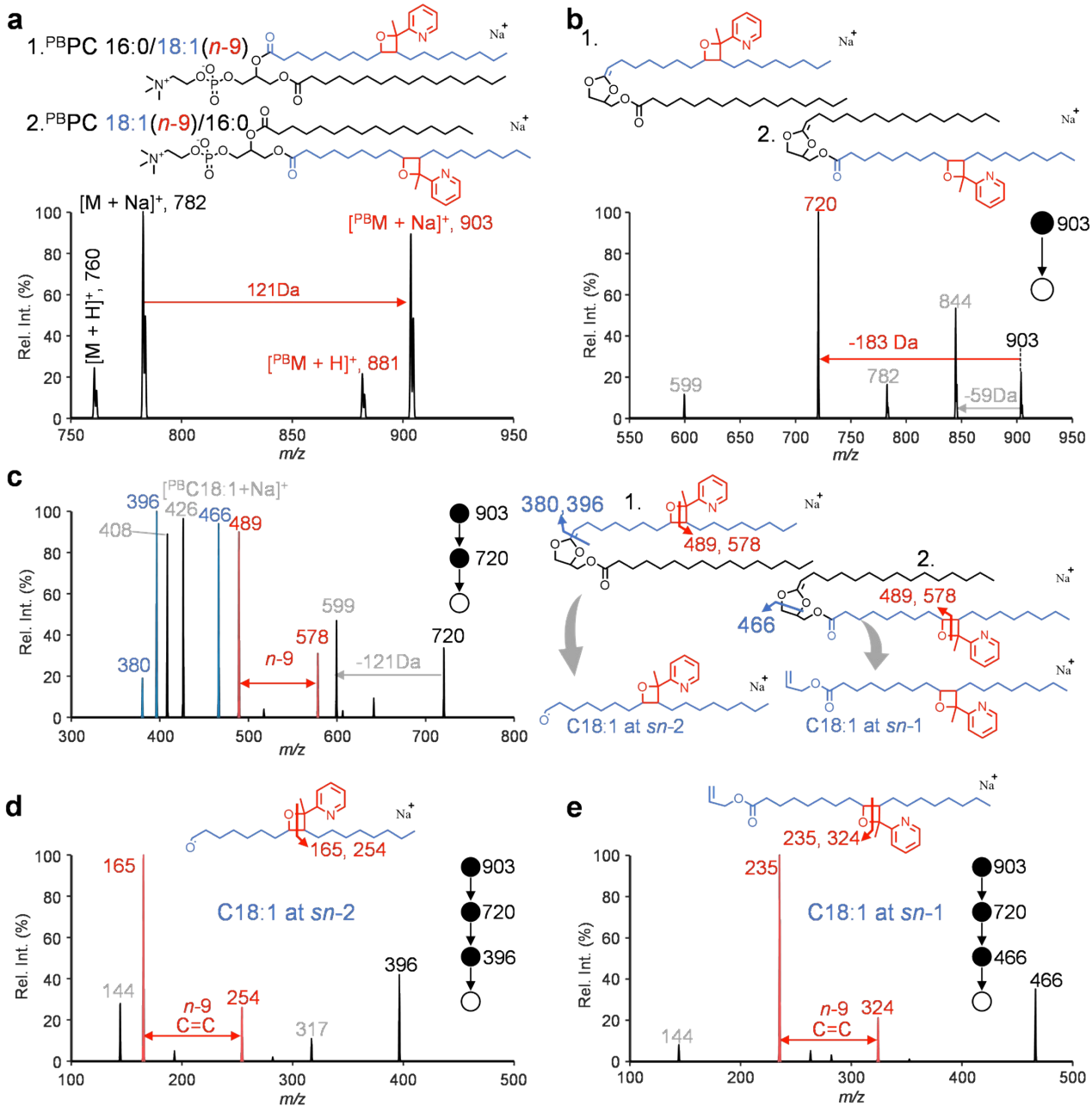

Supplementary Figure 17. Structural elucidation of the mixture of PC 16:0/18:1(*n*-9) and PC 18:1(*n*-9)/16:0 by PB-MS^3 and PB-MS^4 for PB product with added sodium. 5 μM PC 16:0/18:1(*n*-9) + 5 μM PC 18:1(*n*-9)/16:0 + 100μM sodium acetate in acetonitrile/H_2O (1:1, v/v). (a) Scheme for the fragmentation of PB products with added sodium. (b) MS spectrum with added sodium of the mixture after PB reaction. (c) MS/MS spectrum of the PB product with added sodium. (d) Determination of *sn*-position or C=C location by PB-MS^3 for PB product with added sodium. (e-f) Assigning C=C location in *sn*-specific position. (e) Assigning C=C location in *sn*-2, (f) assigning C=C location in *sn*-1.

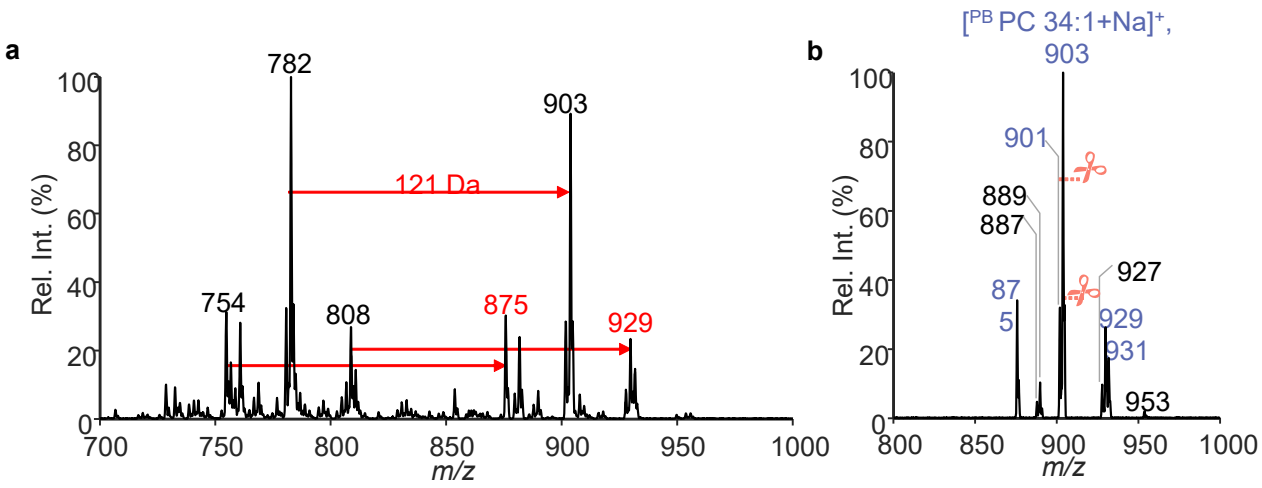

Supplementary Figure 18. The MS spectra of a single MDA-MB-468 cell using methanol/acetonitrile (1:1, v/v) with 100 μM sodium acetate as auxiliary solution. (a) MS spectrum after PB reaction. (b) MS spectrum after accumulation. The 9 PB product peaks were retained, and the top 5 peaks marked in blue font were subjected to MMSPAT to identify the C=C position at the specific *sn*-position.

$$Yield = \frac{\sum Int.\,(^{PB}(precusors))}{\sum Int.\,(^{PB}(precusors)) + \sum Int.(remaining\ precurosrs)}.$$

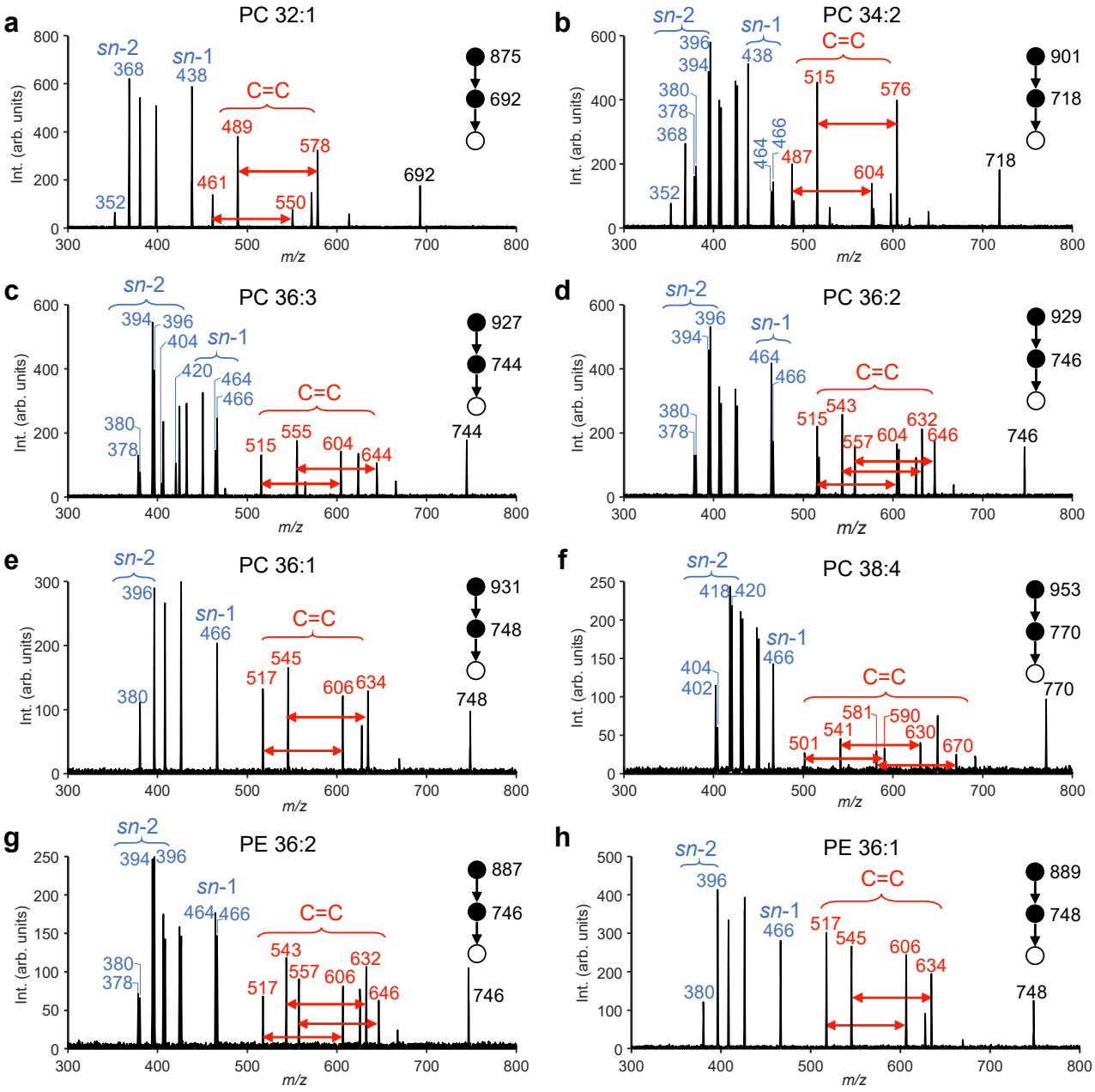

Supplementary Figure 19. MS^3 spectra after PB reaction of a single MDA-MB-468 cell. (a) MS^3 of $[^{PB}PC\ 32:1+Na]^+$. (b) MS^3 of $[^{PB}\ PC\ 34:2+Na]^+$. (c) MS^3 of $[^{PB}\ PC\ 36:3+Na]^+$. (d) MS^3 of $[^{PB}\ PC\ 36:2+Na]^+$. (e) MS^3 of $[^{PB}\ PC\ 36:1+Na]^+$. (f) MS^3 of $[^{PB}\ PC\ 38:4+Na]^+$. (g) MS^3 of $[^{PB}\ PE\ 36:2+Na]^+$. (h) MS^3 of $[^{PB}\ PE\ 36:1+Na]^+$.

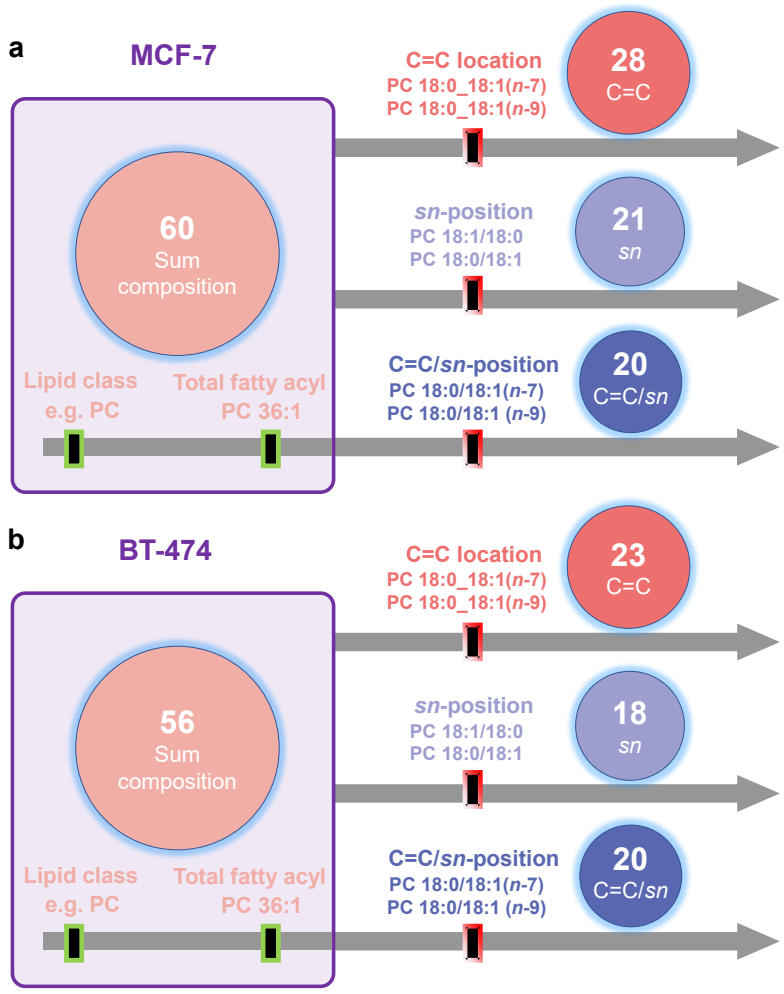

Supplementary Figure 20. Lipid species identified. (a) For a single MCF-7 cell, lipid species identified at the composition, C=C location, *sn*-position, and C=C/*sn*-position. (b) For a single BT-474 cell, lipid species identified at the composition, C=C location, *sn*-position, and C=C/*sn*-position.

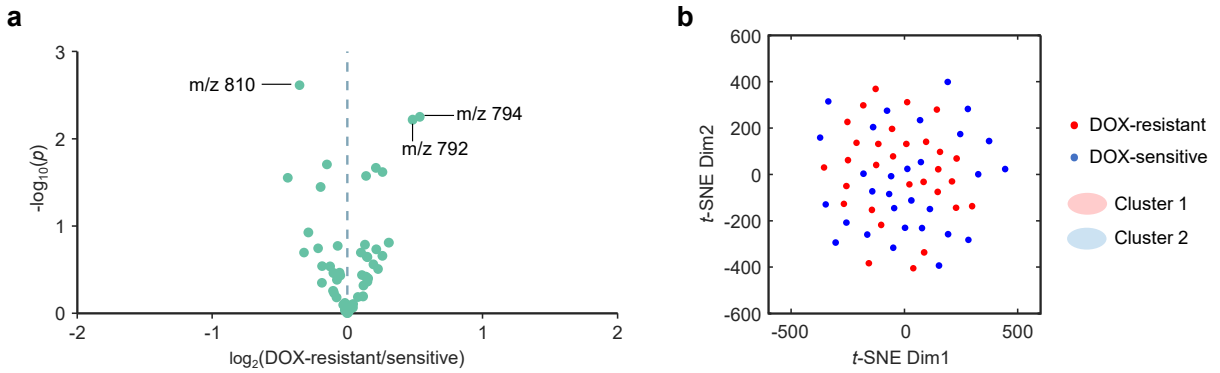

Supplementary Figure 21. Discrimination of DOX-resistant and DOX-sensitive human chronic myelogenous leukemia K562 cells (N=30). *P*-values were determined by two-tailed *t*-test. (a) Alterations of MS1 peak features (normalized to the intensity of *m/z* 760) between DOX-resistant

group cells and DOX-sensitive group cells. *p*-values were determined by two-tailed *t*-test. (b) *t*-SNE plot of DOX-resistant group cells and DOX-sensitive group cells by MS1 peak features (normalized to the intensity of *m/z* 760).

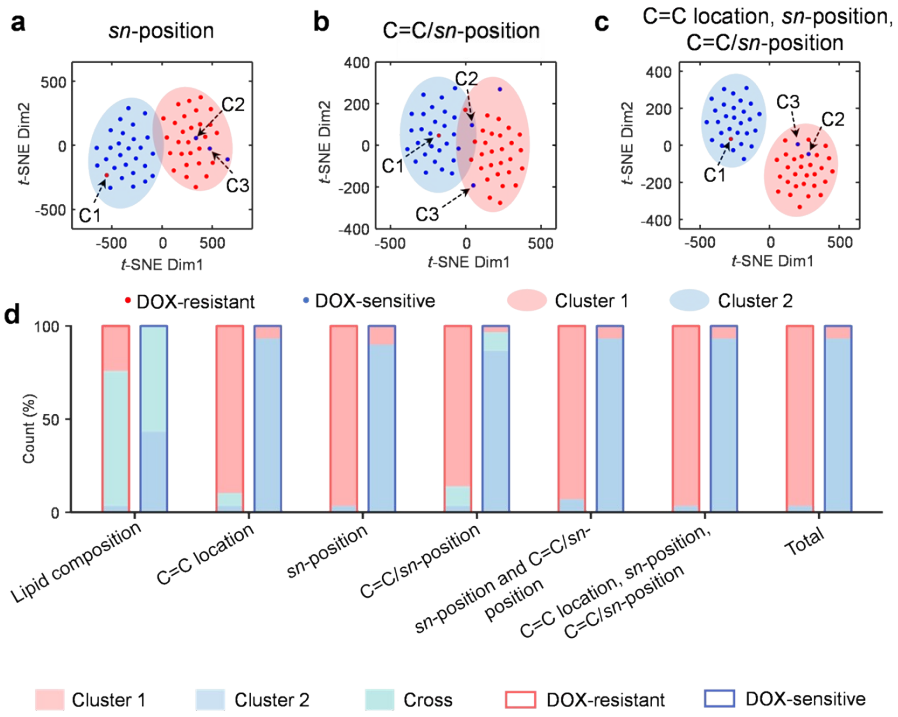

Supplementary Figure 22. Discrimination of DOX-resistant (N=29) and DOX-sensitive (N=30) human chronic myelogenous leukemia K562 cells. (a-c) *t*-SNE plot of DOX-resistant group cells and DOX-sensitive group cells by (a) Ratio of different *sn*-position isomers, (b) Ratio of different C=C/*sn*-position isomers, (c) Ratio of C=C location isomers, ratio of *sn*-position isomers and C=C/*sn*-position isomers. Two cluster areas were circled by k-means clustering results with a confidence probability of 0.95. C1 was cell #8, C2 was cell #33 and C3 was cell #38. (d) Cell number distribution in each cluster.

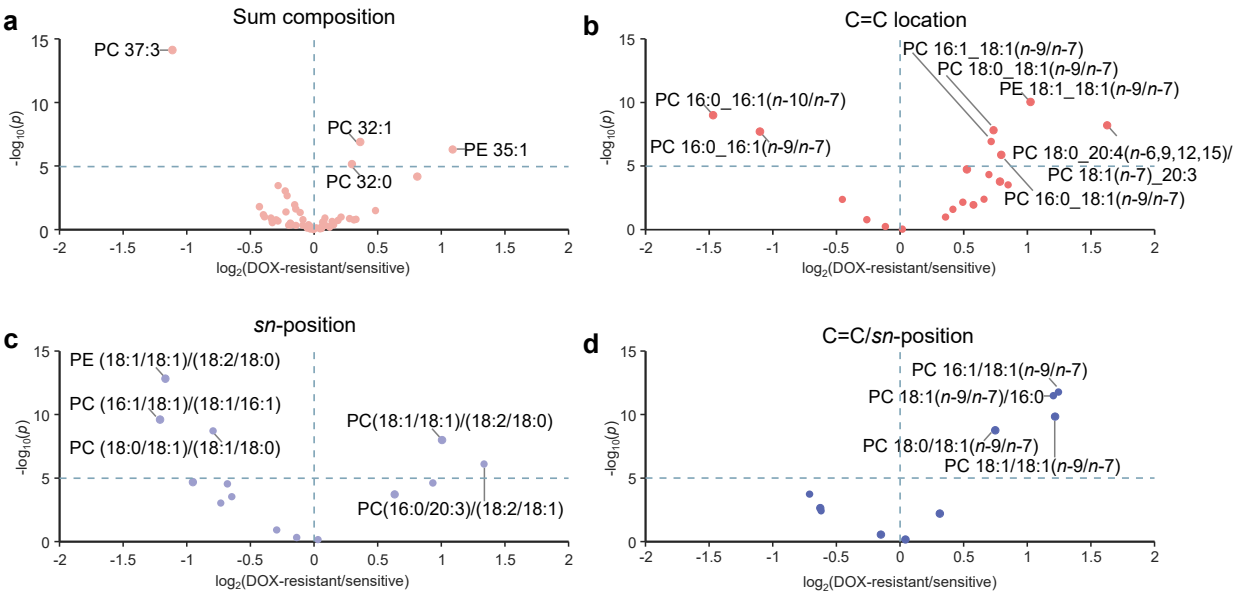

Supplementary Figure 23. (a) Alterations of the sum composition of lipids, (b) ratio of C=C location isomers, (c) ratio of different *sn*-position isomers, and (d) ratio of C=C/*sn*-position isomers. *p*-values were determined by two-tailed *t*-test.

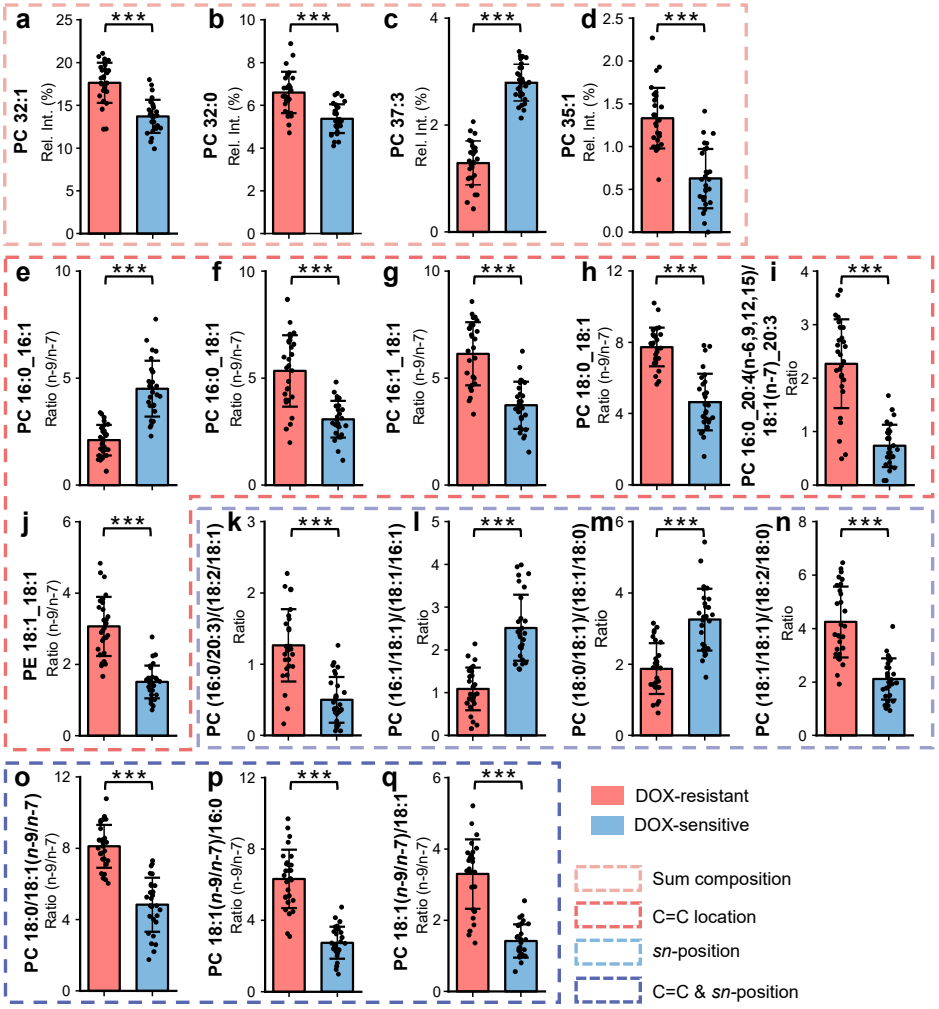

Supplementary Figure 24. Comparison between DOX-resistant group cells (N=28) and DOX-sensitive group cells (N=28). (a-e) Lipid sum composition, including (a) PC 32:1, (b) PC 32:0, (c) PC 34:3, (d) PC 37:3 and (e) PC 35:1. (f-k) C=C location, including (f) PC 16:0_16_1(*n*-9/*n*-7), (g) PC 16:0_18:1(*n*-9/*n*-7), (h) PC 16:1_18:1(*n*-9/*n*-7), (i) PC 18:0_18:1(*n*-9/*n*-7), (j) PC 16:0_20:4(*n*-6,9,12,15)/18:1(*n*-7)_20:3 and (k) PE 18:1_18:1(*n*-9/*n*-7). (l-o) *sn*-position, including (l) PC (16:0/20:3)/(18:2/18:1), (m) PC (16:1/18:1)/(18:1/16:1), (n) PC(18:0/18:1)/(18:1/18:0), and (o) PC(18:1/18:1)/(18:2/18:0). (p-r) C=C/*sn*-position, including (p) PC 18:0/18:1(*n*-9/*n*-7), (q) PC 18:1(*n*-9/*n*-7)/16:0, and (r) PC 18:1(*n*-9/*n*-7)/18:1. ***: $p<0.001$. *p*-values were determined by two-tailed *t*-test. Error bars represent SDs.

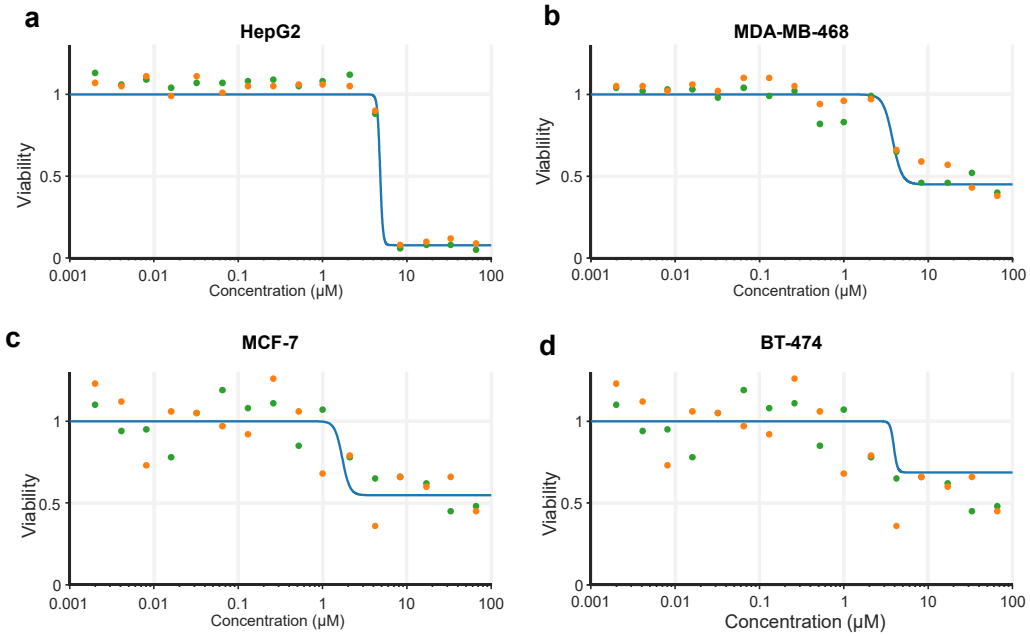

Supplementary Figure 25. Relative viability treated with different concentrations of the ferroptosis inducer Erastin for 24 h (N=2 independent experiments) of (a) HepG2, (b)MDA-MB-468, (c) BT-474 and (d) MCF-7.[5] Source data comes from https://depmap.org/portal/compound/ERASTIN?tab=dose-curves.

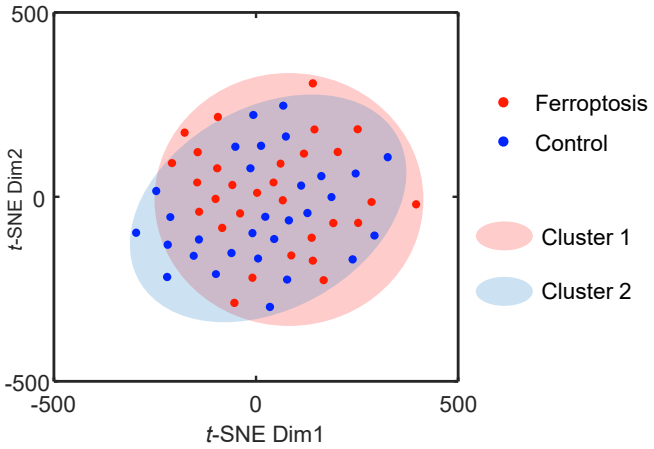

Supplementary Figure 26. *t*-SNE plot using MS/MS analysis results, including the ratio of different lipid sum compositions, the ratio of C=C location isomers, the ratio of different *sn*-position isomers, and the ratio of C=C/*sn*-position isomers. Ferroptosis-induced group cells (N=30) and control group cells (N=30) of MCF-7. Two cluster areas were circled by *k*-means clustering results with a confidence probability of 0.95.

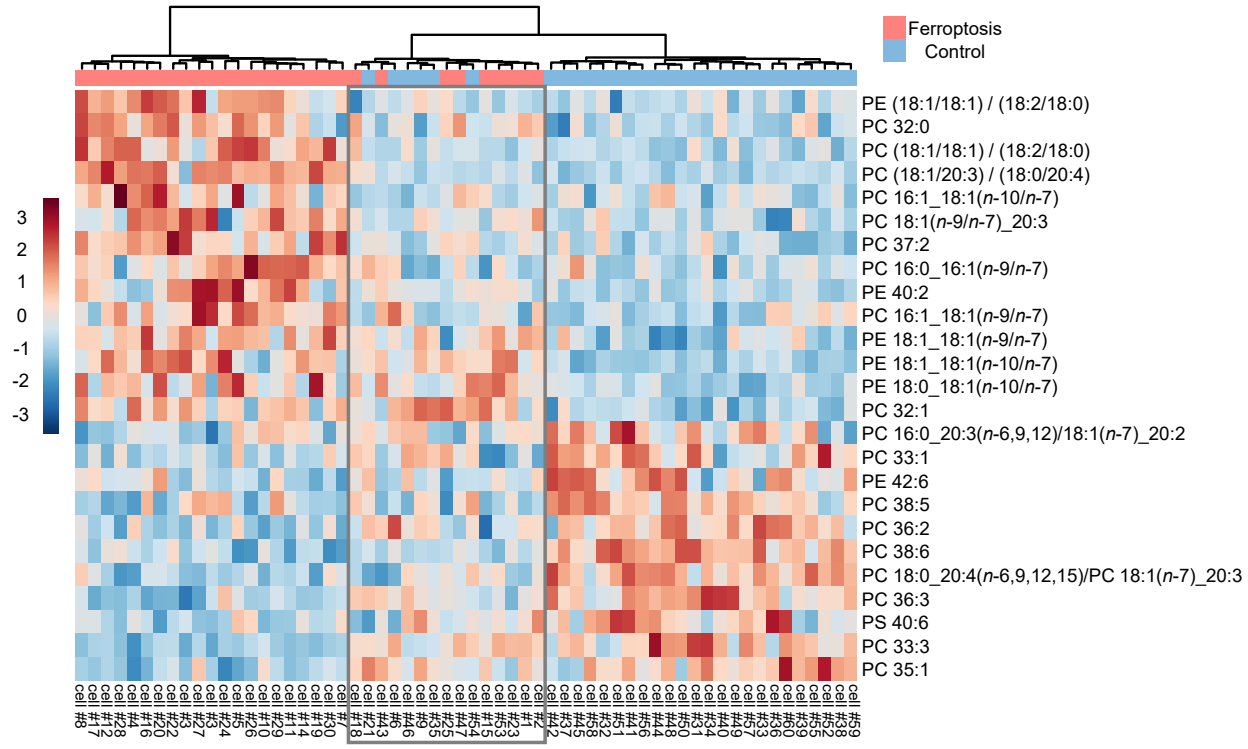

Supplementary Figure 27. Hierarchical cluster analysis of ferroptosis-induced group cells (N=30) and control group cells (N=30) for MDA-MB-468. The gray box represented the intersection of the two types of cells. The top 25 features ranked by –log(*p*) values were used for the cluster. *p*-values were determined by two-tailed *t*-test.

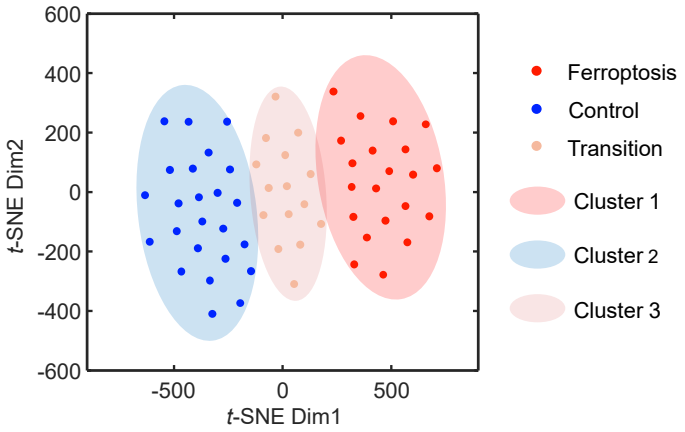

Supplementary Figure 28. *t*-SNE plot of ferroptosis-induced (Ferroptosis) group cells (N=21), cells in Transition state (N=15), and Control group cells (N=24) for MDA-MB-468, using MS/MS analysis results, including lipid sum composition, the ratio of C=C location isomers, the ratio of different *sn*-position isomers, and the ratio of C=C/*sn*-position isomers. Three cluster areas were circled by *k*-means

clustering results with a confidence probability of 0.95.

Below is a comparison our method with other state-of-the-art techniques, including:

a) ID-organic cytoMS (Qin et al., Nat. Commun. 2024): We compare the total number of metabolites identified (150) versus our lipid count (~100), noting that their method is not lipid-specific and provides only sum composition level information, whereas our method achieves deep structural resolution (sn-position, C=C location).

b) Trapped Ion Mobility Spectrometry (TIMS) Imaging (Li et al., Nat. Commun. 2023): We will contrast their identification of 185 lipids at the sum composition level with our ~100 lipids, emphasizing that while their coverage is high, it lacks the structural specificity (C=C location, sn-position) that is central to our study and biological conclusions.

c) On-demand nanoESI with PB reaction (Our previous work, Li et al., Nat. Commun. 2021): We will explicitly compare this prior approach, which first introduced C=C location analysis for single cells. We will demonstrate that the dual-LIT platform significantly enhances coverage (from ~30 lipids with C=C specificity to ~100 total lipids, including 30 with C=C location) and enables more complex analyses (sn-position, C=C/sn-position) that were previously infeasible due to ion limitations.

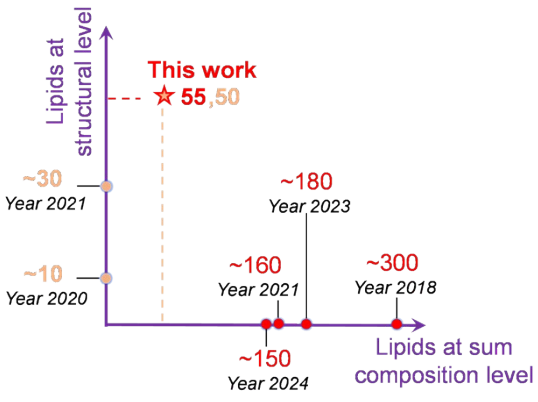

Supplementary Figure 29. Comparison between our work with other works. The horizontal axis represents the number of identified lipids at sum composition level, and the vertical axis represents the number of identified lipids at structural level (C=C position or sn-position), excluding duplicate lipid molecules.

Supplementary Table 1. Lipids in single MDA-MB-468 cells identified by the tandem MS with miniature dual-LIT MS

No.	Name	Adduct	*m/z*	MS/MS Fragments
1	**PC 30:0**	M+H	706	184
2	**PC 31:2**	M+H	716	184
3	**PC 31:1**	M+H	718	184
4	**PC 31:0**	M+H	720	184
5	**PC 32:2**	M+H	730	184
6	**PC 32:1**	M+H	732	184
7	**PC 32:0**	M+H	734	184
8	**PC 33:3**	M+H	742	184
9	**PC 33:2**	M+H	744	184
10	**PC 33:1**	M+H	746	184
11	**PC 33:0**	M+H	748	184
12	**PC 34:3**	M+H	756	184
13	**PC 34:2**	M+H	758	184
14	**PC 34:1**	M+H	760	184
15	**PC 34:0**	M+H	762	184
16	**PC 35:2**	M+H	772	184
17	**PC 35:1**	M+H	774	184
18	**PC 35:0**	M+H	776	184
19	**PC 36:3**	M+H	784	184
20	**PC 36:2**	M+H	786	184
21	**PC 36:1**	M+H	788	184
22	**PC 36:0**	M+H	790	184
23	**PC 37:3**	M+H	798	184
24	**PC 37:2**	M+H	800	184
25	**PC 38:6**	M+H	806	184
26	**PC 38:5**	M+H	808	184
27	**PC 38:4**	M+H	810	184
28	**PC 38:3**	M+H	812	184
29	**PC 38:2**	M+H	814	184
30	**PC 39:4**	M+H	824	184
31	**PC 39:3**	M+H	826	184
32	**PC 40:5**	M+H	836	184
33	**PC 40:4**	M+H	838	184
34	**PC 40:3**	M+H	840	184
35	**PC 40:2**	M+H	842	184
36	**PE 34:2**	M+H	716	575
37	**PE 34:1**	M+H	718	577
38	**PE 34:0**	M+H	720	579
39	**PE 35:2**	M+H	730	589
40	**PE 35:1**	M+H	732	591
41	**PE 35:0**	M+H	734	593
42	**PE 36:3**	M+H	742	601
43	**PE 36:2**	M+H	744	603
44	**PE 36:1**	M+H	746	605
45	**PE 36:0**	M+H	748	607
46	**PE 38:6**	M+H	764	623
47	**PE 38:4**	M+H	768	627
48	**PE 38:2**	M+H	772	631
49	**PE 38:1**	M+H	774	633
50	**PE 40:6**	M+H	792	651
51	**PE 40:3**	M+H	798	657
52	**PE 40:2**	M+H	800	659
53	**PE 42:6**	M+H	820	679
54	**PE 42:4**	M+H	824	683
55	**PE 42:3**	M+H	826	685
56	**PS 36:3**	M+H	786	601
57	**PS 36:2**	M+H	788	603
58	**PS 38:6**	M+H	808	623
59	**PS 38:5**	M+H	810	625
60	**PS 38:4**	M+H	812	627
61	**PS 40:6**	M+H	836	651
62	**PS 40:5**	M+H	838	653
63	**PS 40:4**	M+H	840	655
64	**SM 34:1**	M+H	703	184

Supplementary Table 2**.** Lipid isomers with **C=C locations** in single MDA-MB-468 cells identified by the tandem MS with miniature dual-LIT MS

No.	Name	Adduct	*m/z*	PB product	Diagnostic Ions	C=C location
1					608, 697	**PC 16:0_16:1(*n*-10)**
2	PC 32:1	M+H	732	853	622, 711	**PC 16:0_16:1(*n*-9)**
3					650, 739	**PC 16:0_16:1(*n*-7)**
4					634, 723	**PC 16:1_18:1(*n*-10)**
5	PC 34:2	M+H	758	879	648, 737	**PC 16:1_18:1(*n*-9)**
6					676, 765	**PC 16:1_18:1(*n*-7)**
7					650, 739; 690, 779	**PC 16:0_18:2(*n*-6, 9)**
8					636, 725	**PC 16:0_18:1(*n*-10)**
9	PC 34:1	M+H	760	881	650, 739	**PC 16:0_18:1(*n*-9)**
10					678, 767	**PC 16:0_18:1(*n*-7)**
11					636, 725; 676, 765; 716, 805	**PC 16:0_20:3(*n*-6, 9, 12)**
12	PC 36:3	M+H	784	905	674, 763; 676, 765; 716, 805	**PC 18:1(*n*-9)_18:2(*n*-6, 9)**
13					702, 791; 676, 765; 716, 805	**PC 18:1(*n*-7)_18:2(*n*-6, 9)**
14					678,767;718,807	**PC 18:0_18:2(*n*-6,9)**
15	PC 36:2	M+H	786	907	662, 751	**PC 18:1_18:1(*n*-10)**
16					676, 765	**PC 18:1_18:1(*n*-9)**
17					704, 793	**PC 18:1_18:1(*n*-7)**
18					664, 753	**PC 18:0_18:1(*n*-10)**
19	PC 36:1	M+H	788	909	678, 767	**PC 18:0_18:1(*n*-9)**
20					706, 795	**PC 18:0_18:1(*n*-7)**
21					700, 789; 662, 751; 702, 791; 742, 831	**PC 18:1(*n*-9)_20:3(*n*-6, 9, 12)**
22	PC 38:4	M+H	810	931	728, 817; 662, 751; 702, 791; 742, 831	**PC 18:1(*n*-7)_20:3(*n*-6, 9, 12)**
23					622, 711; 662, 751; 702, 791; 742, 831	**PC 18:0_20:4(*n*-6, 9, 12, 15)**
24					495, 584; 535, 624	**PE 18:0_18:2(*n*-6, 9)**
25	PE 36:2	M+H	744	865	479, 568	**PE 18:1_18:1(*n*-10)**
26					493, 582	**PE 18:1_18:1(*n*-9)**
27					521, 610	**PE 18:1_18:1(*n*-7)**
28					481, 570	**PE 18:0_18:1(*n*-10)**
29	PE 36:1	M+H	746	867	495, 584	**PE 18:0_18:1(*n*-9)**
30					523, 612	**PE 18:0_18:1(*n*-7)**

Supplementary Table 3. Lipid isomers with *sn*-positions in single MDA-MB-468 cells identified by the tandem MS with miniature dual-LIT MS

No.	Name	Adduct	*m/z*	PB product	Diagnostic Ions	*sn*-position
1	PC 32:1	M+Na	754	875	352, 368	**PC16:0/16:1**
2					438	**PC16:1/16:0**
3	PC 34:2	M+Na	780	901	380, 396, 438	**PC 16:1/18:1**
4					352, 368, 466	**PC 18:1/16:1**
5					378, 394	**PC 16:0/18:2**
6					464	**PC 18:2/16:0**
7	PC 34:1	M+Na	782	903	380, 396	**PC 16:0/18:1**
8					466	**PC 18:1/16:0**
9	PC 36:3	M+Na	806	927	404, 420	**PC 16:0/20:3**
10					378, 394, 466	**PC 18:1/18:2**
11					380, 396, 464	**PC 18:2/18:1**
12	PC 36:2	M+Na	808	929	380, 396, 466	**PC 18:1/18:1**
13					378, 394	**PC 18:0/18:2**
14					464	**PC 18:2/18:0**
15	PC 36:1	M+Na	810	931	380, 396	**PC 18:0/18:1**
16					466	**PC 18:1/18:0**
17	PC 38:4	M+Na	832	953	404, 420, 466	**PC 18:1/20:3**
18					402, 418	**PC 18:0/20:4**
19	PE 36:2	M+Na	766	887	380, 396, 466	**PE 18:1/18:1**
20					378, 394	**PE 18:0/18:2**
21					464	**PE 18:2/18:0**
22	PE 36:1	M+Na	768	889	380, 396	**PE 18:0/18:1**
23					466	**PE 18:1/18:0**

Supplementary Table 4. Lipid isomers with C=C locations in *sn*-2 or *sn*-1 positions in single cells, including MDA-MB-468, MCF-7, BT-474, K562, and HepG2, identified by the tandem MS with miniature dual-LIT MS

Species	C=C location	Diagnostic Ions
PC 16:0/**16:1**	*n*-9	137, 226
	n-7	165, 254
PC **16:1**/16:0	*n*-9	207, 296
	n-7	235, 324
PC 16:1/**18:1**	*n*-9	165, 254
	n-7	193, 282
PC **18:1**/16:1	*n*-9	235, 324
	n-7	263, 352
PC 16:0/**18:1**	*n*-9	165, 254
	n-7	193, 282
PC **18:1**/16:0	*n*-9	235, 324
	n-7	263, 352
PC 18:1/**18:1**	*n*-9	165, 254
	n-7	193, 282
PC **18:1**/18:1	*n*-9	235, 324
	n-7	263, 352
PC 18:0/**18:1**	*n*-9	165, 254
	n-7	193, 282
PC **18:1**/18:0	*n*-9	235, 324
	n-7	263, 352

Supplementary Table 5. Lipids in single MCF-7 cells identified by the tandem MS with miniature dual-LIT MS

No.	Name	Adduct	*m/z*	MS/MS Fragments
1	**PC 30:0**	M+H	706	184
2	**PC 31:1**	M+H	718	184
3	**PC 31:0**	M+H	720	184
4	**PC 32:2**	M+H	730	184
5	**PC 32:1**	M+H	732	184
6	**PC 32:0**	M+H	734	184
7	**PC 33:2**	M+H	744	184
8	**PC 33:1**	M+H	746	184
9	**PC 33:0**	M+H	748	184
10	**PC 34:3**	M+H	756	184
11	**PC 34:2**	M+H	758	184
12	**PC 34:1**	M+H	760	184
13	**PC 34:0**	M+H	762	184
14	**PC 35:2**	M+H	772	184
15	**PC 35:1**	M+H	774	184
16	**PC 35:0**	M+H	776	184
17	**PC 36:3**	M+H	784	184
18	**PC 36:2**	M+H	786	184
19	**PC 36:1**	M+H	788	184
20	**PC 36:0**	M+H	790	184
21	**PC 37:4**	M+H	796	184
22	**PC 37:3**	M+H	798	184
23	**PC 37:2**	M+H	800	184
24	**PC 38:6**	M+H	806	184
25	**PC 38:5**	M+H	808	184
26	**PC 38:4**	M+H	810	184
27	**PC 38:3**	M+H	812	184
28	**PC 38:2**	M+H	814	184
29	**PC 39:4**	M+H	824	184
30	**PC 39:3**	M+H	826	184

No.	Name	Adduct	*m/z*	MS/MS Fragments
31	**PC 40:5**	M+H	836	184
32	**PC 40:4**	M+H	838	184
33	**PC 40:3**	M+H	840	184
34	**PC 40:2**	M+H	842	184
35	**PE 34:1**	M+H	718	577
36	**PE 34:0**	M+H	720	579
37	**PE 35:2**	M+H	730	589
38	**PE 35:1**	M+H	732	591
39	**PE 35:0**	M+H	734	593
40	**PE 36:2**	M+H	744	603
41	**PE 36:1**	M+H	746	605
42	**PE 36:0**	M+H	748	607
43	**PE 38:4**	M+H	768	627
44	**PE 38:2**	M+H	772	631
45	**PE 38:1**	M+H	774	633
46	**PE 40:6**	M+H	792	651
47	**PE 40:3**	M+H	798	657
48	**PE 40:2**	M+H	800	659
49	**PE 42:6**	M+H	820	679
50	**PE 42:5**	M+H	822	681
51	**PE 42:4**	M+H	824	683
52	**PS 36:3**	M+H	786	601
53	**PS 36:2**	M+H	788	603
54	**PS 38:6**	M+H	808	623
55	**PS 38:5**	M+H	810	625
56	**PS 38:4**	M+H	812	627
57	**PS 40:6**	M+H	836	651
58	**PS 40:5**	M+H	838	184
59	**PS 40:4**	M+H	840	655
60	**SM 34:1**	M+H	703	184

Supplementary Table 6. Lipid isomers with C=C locations in single MCF-7 cells identified by the tandem MS with miniature dual-LIT MS

No.	Name	Adduct	*m/z*	PB product	Diagnostic Ions	C=C location
1	PC 32:2	M+H	730	851	620, 709	**PC 16:1_16:1(*n*-9)**
2					648, 737	**PC 16:1_16:1(*n*-7)**
3	PC 32:1	M+H	732	853	608, 697	**PC 16:0_16:1(*n*-10)**
4					622, 711	**PC 16:0_16:1(*n*-9)**
5					650, 739	**PC 16:0_16:1(*n*-7)**
6	PC 34:2	M+H	758	879	634, 723	**PC 16:1_18:1(*n*-10)**
7					648, 737	**PC 16:1_18:1(*n*-9)**
8					676, 765	**PC 16:1_18:1(*n*-7)**
9					650, 739; 690, 779	**PC 16:0_18:2(*n*-6, 9)**
10	PC 34:1	M+H	760	881	636, 725	**PC 16:0_18:1(*n*-10)**
11					650, 739	**PC 16:0_18:1(*n*-9)**
12					678, 767	**PC 16:0_18:1(*n*-7)**
13	PC 36:3	M+H	784	905	636, 725; 676, 765; 716, 805	**PC 16:0_20:3(*n*-6, 9, 12)**
14					674, 763; 676, 765; 716, 805	**PC 18:1(*n*-9)_18:2(*n*-6, 9)**
15					702, 791; 676, 765; 716, 805	**PC 18:1(*n*-7)_18:2(*n*-6, 9)**
16	PC 36:2	M+H	786	907	678,767;718,807	**PC 18:0_18:2(*n*-6,9)**
17					662, 751	**PC 18:1_18:1(*n*-10)**
18					676, 765	**PC 18:1_18:1(*n*-9)**
19					704, 793	**PC 18:1_18:1(*n*-7)**
20	PC 36:1	M+H	788	909	664, 753	**PC 18:0_18:1(*n*-10)**
21					678, 767	**PC 18:0_18:1(*n*-9)**
22					706, 795	**PC 18:0_18:1(*n*-7)**
23	PC 38:5	M+H	808	929	698, 787; 620,709;660, 749; 700, 789; 740, 829	**PC 18:1(*n*-9)_20:4(*n*-6, 9, 12, 15)**
24					726, 815; 620,709; 660, 749; 700, 789; 740, 829	**PC 18:1(*n*-7)_20:4(*n*-6, 9, 12, 15)**
25					622, 711; 662, 751; 702, 791; 742, 831;782,871	**PC 18:0_20:5(*n*-3, 6, 9, 12, 15)**
26	PE 36:1	M+H	746	867	481, 570	**PE 18:0_18:1(*n*-10)**
27					495, 584	**PE 18:0_18:1(*n*-9)**
28					523, 612	**PE 18:0_18:1(*n*-7)**

Supplementary Table 7. Lipid isomers with *sn*-positions in single MCF-7 cells identified by the tandem MS with miniature dual-LIT MS

No.	Name	Adduct	*m/z*	PB product	Diagnostic Ions	*sn*-position
1	PC 32:2	M+Na	752	873	352, 368, 438	**PC 16:1/16:1**
2	PC 32:1	M+Na	754	875	352, 368	**PC16:0/16:1**
3					438	**PC16:1/16:0**
4	PC 34:2	M+Na	780	901	380, 396, 438	**PC 16:1/18:1**
5					352, 368, 466	**PC 18:1/16:1**
6					378, 394	**PC 16:0/18:2**
7					464	**PC 18:2/16:0**
8	PC 34:1	M+Na	782	903	380, 396	**PC 16:0/18:1**
9					466	**PC 18:1/16:0**
10	PC 36:3	M+Na	806	927	404, 420	**PC 16:0/20:3**
11					378, 394, 466	**PC 18:1/18:2**
12					380, 396, 464	**PC 18:2/18:1**
13	PC 36:2	M+Na	808	929	380, 396, 466	**PC 18:1/18:1**
14					378, 394	**PC 18:0/18:2**
15					464	**PC 18:2/18:0**
16	PC 36:1	M+Na	810	931	380, 396	**PC 18:0/18:1**
17					466	**PC 18:1/18:0**
18	PC 38:5	M+Na	830	951	402, 418, 466	**PC 18:1/20:4**
19					400, 416	**PC 18:0/20:5**
20	PE 36:1	M+Na	768	889	380, 396	**PE 18:0/18:1**
21					466	**PE 18:1/18:0**

Supplementary Table 8. Lipids in single BT-474 cells identified by the tandem MS with miniature dual-LIT MS

No.	Name	Adduct	*m/z*	MS/MS Fragments
1	**PC 30:0**	M+H	706	184
2	**PC 31:1**	M+H	718	184
3	**PC 31:0**	M+H	720	184
4	**PC 32:2**	M+H	730	184
5	**PC 32:1**	M+H	732	184
6	**PC 32:0**	M+H	734	184
7	**PC 33:2**	M+H	744	184
8	**PC 33:1**	M+H	746	184
9	**PC 33:0**	M+H	748	184
10	**PC 34:3**	M+H	756	184
11	**PC 34:2**	M+H	758	184
12	**PC 34:1**	M+H	760	184
13	**PC 34:0**	M+H	762	184
14	**PC 35:2**	M+H	772	184
15	**PC 35:1**	M+H	774	184
16	**PC 35:0**	M+H	776	184
17	**PC 36:3**	M+H	784	184
18	**PC 36:2**	M+H	786	184
19	**PC 36:1**	M+H	788	184
20	**PC 36:0**	M+H	790	184
21	**PC 37:2**	M+H	800	184
22	**PC 38:6**	M+H	806	184
23	**PC 38:5**	M+H	808	184
24	**PC 38:4**	M+H	810	184
25	**PC 38:3**	M+H	812	184
26	**PC 38:2**	M+H	814	184
27	**PC 39:4**	M+H	824	184
28	**PC 39:3**	M+H	826	184

No.	Name	Adduct	*m/z*	MS/MS Fragments
29	**PC 40:5**	M+H	836	184
30	**PC 40:4**	M+H	838	184
31	**PC 40:3**	M+H	840	184
32	**PC 40:2**	M+H	842	184
33	**PE 34:2**	M+H	718	577
34	**PE 34:0**	M+H	720	579
35	**PE 35:2**	M+H	730	589
36	**PE 35:1**	M+H	732	591
37	**PE 36:2**	M+H	744	603
38	**PE 36:1**	M+H	746	605
39	**PE 36:0**	M+H	748	607
40	**PE 38:4**	M+H	768	627
41	**PE 38:2**	M+H	772	631
42	**PE 38:1**	M+H	774	633
43	**PE 40:6**	M+H	792	651
44	**PE 40:3**	M+H	798	657
45	**PE 40:2**	M+H	800	659
46	**PE 42:6**	M+H	820	679
47	**PE 42:4**	M+H	824	683
48	**PE 42:3**	M+H	826	685
49	**PS 36:3**	M+H	786	601
50	**PS 36:2**	M+H	788	603
51	**PS 38:6**	M+H	808	623
52	**PS 38:5**	M+H	810	625
53	**PS 38:4**	M+H	812	627
54	**PS 40:5**	M+H	838	653
55	**PS 40:4**	M+H	840	655
56	**SM 34:1**	M+H	703	184

Supplementary Table 9. Lipid isomers with C=C locations in single BT-474 cells identified by the tandem MS with miniature dual-LIT MS

No.	Name	Adduct	*m/z*	PB product	Diagnostic Ions	C=C location
1	PC 32:1	M+H	732	853	608, 697	**PC 16:0_16:1(*n*-10)**
2					622, 711	**PC 16:0_16:1(*n*-9)**
3					650, 739	**PC 16:0_16:1(*n*-7)**
4	PC 34:2	M+H	758	879	634, 723	**PC 16:1_18:1(*n*-10)**
5					648, 737	**PC 16:1_18:1(*n*-9)**
6					676, 765	**PC 16:1_18:1(*n*-7)**
7					650, 739; 690, 779	**PC 16:0_18:2(*n*-6, 9)**
8	PC 34:1	M+H	760	881	636, 725	**PC 16:0_18:1(*n*-10)**
9					650, 739	**PC 16:0_18:1(*n*-9)**
10					678, 767	**PC 16:0_18:1(*n*-7)**
11	PC 36:3	M+H	784	905	636, 725; 676, 765; 716, 805	**PC 16:0_20:3(*n*-6, 9, 12)**
12					674, 763; 676, 765; 716, 805	**PC 18:1(*n*-9)_18:2(*n*-6, 9)**
13					702, 791; 676, 765; 716, 805	**PC 18:1(*n*-7)_18:2(*n*-6, 9)**
14	PC 36:2	M+H	786	907	678,767;718,807	**PC 18:0_18:2(*n*-6,9)**
15					662, 751	**PC 18:1_18:1(*n*-10)**
16					676, 765	**PC 18:1_18:1(*n*-9)**
17					704, 793	**PC 18:1_18:1(*n*-7)**
18	PC 36:1	M+H	788	909	664, 753	**PC 18:0_18:1(*n*-10)**
19					678, 767	**PC 18:0_18:1(*n*-9)**
20					706, 795	**PC 18:0_18:1(*n*-7)**
21	PE 36:1	M+H	746	867	481, 570	**PE 18:0_18:1(*n*-10)**
22					495, 584	**PE 18:0_18:1(*n*-9)**
23					523, 612	**PE 18:0_18:1(*n*-7)**

Supplementary Table 10. Lipid isomers with *sn*-positions in single BT-474 cells identified by the tandem MS with miniature dual-LIT MS

No.	Name	Adduct	*m/z*	PB product	Diagnostic Ions	*sn*-position
1	PC 32:1	M+Na	754	875	352, 368	**PC16:0/16:1**
2					438	**PC16:1/16:0**
3	PC 34:2	M+Na	780	901	380, 396, 438	**PC 16:1/18:1**
4					352, 368, 466	**PC 18:1/16:1**
5					378, 394	**PC 16:0/18:2**
6					464	**PC 18:2/16:0**
7	PC 34:1	M+Na	782	903	380, 396	**PC 16:0/18:1**
8					466	**PC 18:1/16:0**
9	PC 36:3	M+Na	806	927	404, 420	**PC 16:0/20:3**
10					378, 394, 466	**PC 18:1/18:2**
11					380, 396, 464	**PC 18:2/18:1**
12	PC 36:2	M+Na	808	929	380, 396, 466	**PC 18:1/18:1**
13					378, 394	**PC 18:0/18:2**
14					464	**PC 18:2/18:0**
15	PC 36:1	M+Na	810	931	380, 396	**PC 18:0/18:1**
16					466	**PC 18:1/18:0**
17	PE 36:1	M+Na	768	889	380, 396	**PE 18:0/18:1**
18					466	**PE 18:1/18:0**

Supplementary Table 11. Lipids in single K562 cells identified by the tandem MS with miniature dual-LIT MS

No.	Name	Adduct	*m/z*	MS/MS Fragments
1	**PC 30:0**	M+H	706	184
2	**PC 31:1**	M+H	718	184
3	**PC 32:2**	M+H	730	184
4	**PC 32:1**	M+H	732	184
5	**PC 32:0**	M+H	734	184
6	**PC 33:2**	M+H	744	184
7	**PC 33:1**	M+H	746	184
8	**PC 33:0**	M+H	748	184
9	**PC 34:3**	M+H	756	184
10	**PC 34:2**	M+H	758	184
11	**PC 34:1**	M+H	760	184
12	**PC 34:0**	M+H	762	184
13	**PC 35:2**	M+H	772	184
14	**PC 35:1**	M+H	774	184
15	**PC 35:0**	M+H	776	184
16	**PC 36:3**	M+H	784	184
17	**PC 36:2**	M+H	786	184
18	**PC 36:1**	M+H	788	184
19	**PC 36:0**	M+H	790	184
20	**PC 37:3**	M+H	798	184
21	**PC 37:2**	M+H	800	184
22	**PC 38:6**	M+H	806	184
23	**PC 38:5**	M+H	808	184
24	**PC 38:4**	M+H	810	184
25	**PC 38:3**	M+H	812	184
26	**PC 39:4**	M+H	824	184
27	**PC 39:3**	M+H	826	184
28	**PC 40:5**	M+H	836	184
29	**PC 40:4**	M+H	838	184
30	**PC 40:3**	M+H	840	184
31	**PE 34:1**	M+H	718	577
32	**PE 35:2**	M+H	730	589
33	**PE 35:1**	M+H	732	591
34	**PE 36:2**	M+H	744	603
35	**PE 36:1**	M+H	746	605
36	**PE 36:0**	M+H	748	607
37	**PE 38:2**	M+H	772	631
38	**PE 38:1**	M+H	774	633
39	**PE 40:6**	M+H	792	651
40	**PE 40:3**	M+H	798	657
41	**PE 40:2**	M+H	800	659
42	**PE 42:6**	M+H	820	679
43	**PE 42:4**	M+H	824	683
44	**PE 42:3**	M+H	826	685
45	**PS 36:3**	M+H	786	601
46	**PS 36:2**	M+H	788	603
47	**PS 38:6**	M+H	808	623
48	**PS 38:5**	M+H	810	625
49	**PS 38:4**	M+H	812	627
50	**PS 40:6**	M+H	836	651
51	**PS 40:5**	M+H	838	653
52	**PS 40:4**	M+H	840	655

Supplementary Table 12. Lipid isomers with C=C locations in single K562 cells identified by the tandem MS with miniature dual-LIT MS

No.	Name	Adduct	*m/z*	PB product	Diagnostic Ions	C=C location
1	PC 32:1	M+H	732	853	608, 697	**PC 16:0_16:1(*n*-10)**
2					622, 711	**PC 16:0_16:1(*n*-9)**
3					650, 739	**PC 16:0_16:1(*n*-7)**
4	PC 34:2	M+H	759	879	634, 723	**PC 16:1_18:1(*n*-10)**
5					648, 737	**PC 16:1_18:1(*n*-9)**
6					676, 765	**PC 16:1_18:1(*n*-7)**
7					650, 739; 690, 779	**PC 16:0_18:2(*n*-6, 9)**
8	PC 34:1	M+H	760	881	636, 725	**PC 16:0_18:1(*n*-10)**
9					650, 739	**PC 16:0_18:1(*n*-9)**
10					678, 767	**PC 16:0_18:1(*n*-7)**
11	PC 36:3	M+H	784	905	636, 725; 676, 765; 716, 805	**PC 16:0_20:3(*n*-6, 9, 12)**
12					674, 763; 676, 765; 716, 805	**PC 18:1(*n*-9)_18:2(*n*-6, 9)**
13					702, 791; 676, 765; 716, 805	**PC 18:1(*n*-7)_18:2(*n*-6, 9)**
14	PC 36:2	M+H	786	907	678,767;718,807	**PC 18:0_18:2(*n*-6,9)**
15					662, 751	**PC 18:1_18:1(*n*-10)**
16					676, 765	**PC 18:1_18:1(*n*-9)**
17					704, 793	**PC 18:1_18:1(*n*-7)**
18	PC 36:1	M+H	788	909	664, 753	**PC 18:0_18:1(*n*-10)**
19					678, 767	**PC 18:0_18:1(*n*-9)**
20					706, 795	**PC 18:0_18:1(*n*-7)**
21	PC 38:4	M+H	810	931	700, 789; 662, 751; 702, 791; 742, 831	**PC 18:1(*n*-9)_20:3(*n*-6, 9, 12)**
22					728, 817; 662, 751; 702, 791; 742, 831	**PC 18:1(*n*-7)_20:3(*n*-6, 9, 12)**
23					622, 711; 662, 751; 702, 791; 742, 831	**PC 18:0_20:4(*n*-6, 9, 12, 15)**
24	PE 36:2	M+H	744	865	495, 584; 535, 624	**PE 18:0_18:2(*n*-6, 9)**
25					479, 568	**PE 18:1_18:1(*n*-10)**
26					493, 582	**PE 18:1_18:1(*n*-9)**
27					521, 610	**PE 18:1_18:1(*n*-7)**
28	PE 36:1	M+H	746	867	481, 570	**PE 18:0_18:1(*n*-10)**
29					495, 584	**PE 18:0_18:1(*n*-9)**
30					523, 612	**PE 18:0_18:1(*n*-7)**

Supplementary Table 13. Lipid isomers with *sn*-positions in single K562 cells identified by the tandem MS with miniature dual-LIT MS

No.	Name	Adduct	*m/z*	PB product	Diagnostic Ions	*sn*-position
1	PC 32:1	M+Na	754	875	352, 368	**PC16:0/16:1**
2					438	**PC16:1/16:0**
3	PC 34:2	M+Na	780	901	380, 396, 438	**PC 16:1/18:1**
4					352, 368, 466	**PC 18:1/16:1**
5					378, 394	**PC 16:0/18:2**
6					464	**PC 18:2/16:0**
7	PC 34:1	M+Na	782	903	380, 396	**PC 16:0/18:1**
8					466	**PC 18:1/16:0**
9	PC 36:3	M+Na	806	927	404, 420	**PC 16:0/20:3**
10					378, 394, 466	**PC 18:1/18:2**
11					380, 396, 464	**PC 18:2/18:1**
12	PC 36:2	M+Na	808	929	380, 396, 466	**PC 18:1/18:1**
13					378, 394	**PC 18:0/18:2**
14					464	**PC 18:2/18:0**
15	PC 36:1	M+Na	810	931	380, 396	**PC 18:0/18:1**
16					466	**PC 18:1/18:0**
17	PC 38:4	M+Na	832	953	404, 420, 466	**PC 18:1/20:3**
18					402, 418	**PC 18:0/20:4**
19	PE 36:2	M+Na	766	887	380, 396, 466	**PE 18:1/18:1**
20					378, 394	**PE 18:0/18:2**
21					464	**PE 18:2/18:0**
22	PE 36:1	M+Na	768	889	380, 396	**PE 18:0/18:1**
23					466	**PE 18:1/18:0**

Supplementary Table 14. Definition of lipid ratio

Ratio	Definition
PC 16:0_16:1(*n*-10/*n*-7)	I(608)+I(697) / I(650)+I(739)
PC 16:0_16:1(*n*-9/*n*-7)	I(622)+I(711) / I(650)+I(739)
PC 16:0_18:2(*n*-6,9)/16:1_18:1(*n*-7)	I(650)+I(739)+I(690)+I(779) / I(676)+I(765)
PC 16:1_18:1(*n*-10/*n*-7)	I(634)+I(723) / I(676)+I(765)
PC 16:1_18:1(*n*-9/*n*-7)	I(648)+I(737) / I(676)+I(765)
PC 16:0_18:1(*n*-10/*n*-7)	I(636)+I(725) / I(678)+I(767)
PC 16:0_18:1(*n*-9/*n*-7)	I(650)+I(739) / I(678)+I(767)
PC 16:0_20:3(*n*-6,9,12)/PC 18:1(*n*-7)_18:2	I(636)+I(725) / I(702)+I(791)
PC 18:1(*n*-9/*n*-7)_18:2(*n*-6,9)	I(674)+I(763) / I(702)+I(791)
PC 18:0_18:2(*n*-6,9)/ PC 18:1_18:1((*n*-7))	I(678)+I(767)+I(718)+I(807) / I(704)+I(793)
PC 18:1_18:1(*n*-10/*n*-7)	I(662)+I(751) / I(704)+I(793)
PC 18:1_18:1(*n*-9/*n*-7)	I(676)+I(765) / I(704)+I(793)
PC 18:0_18:1(*n*-10/*n*-7)	I(664)+I(753) / I(706)+I(795)
PC 18:0_18:1(*n*-9/*n*-7)	I(678)+I(767) / I(706)+I(795)
PC 18:0_20:4(*n*-6, 9, 12, 15)/PC 18:1(*n*-7)_20:3	I(622)+I(711) / I(728)+I(817)
PC 18:1(*n*-9/*n*-7)_20:3	I(700)+I(789) / I(728)+I(817)
PE 18:0_18:2(*n*-6, 9)/PE 18:0_18:1(*n*-7)	I(495)+I(584)+I(535)+I(624) / I(521)+I(610)
PE 18:1_18:1(*n*-10/*n*-7)	I(479)+I(568) / I(521)+I(610)
PE 18:1_18:1(*n*-9/*n*-7)	I(493)+I(582) / I(521)+I(610)
PE 18:0_18:1(*n*-10/*n*-7)	I(481)+I(570) / I(523)+I(612)
PE 18:0_18:1(*n*-9/*n*-7)	I(495)+I(584) / I(523)+I(612)
PC (16:0/16:1)/(16:1/16:0)	I(352)+I(368) / I(438)
PC (16:1/18:1)/(18:1/16:1)	I(380)+I(396)+I(438) / I(352)+I(368)+I(466)
PC (16:0/18:2)/(18:1/16:1)	I(378)+I(394) / I(352)+I(368)+I(466)
PC (16:0/18:2)/(18:2/16:0)	I(378)+I(394) / I(464)
PC (16:0/18:1)/(18:1/16:0)	I(380)+I(396) / I(466)
PC(16:0/20:3)/(18:2/18:1)	I(404)+I(420) / I(380)+I(396)+I(464)
PC (18:1/18:2)/(18:2/18:1)	I(378)+I(394)+I(466) / I(380)+I(396)+I(464)
PC(18:1/18:1)/(18:2/18:0)	I(380)+I(396)+I(466) / I(464)
PC (18:0/18:2)/(18:2/18:0)	I(378)+I(394) / I(464)
PC (18:0/18:1)/(18:1/18:0)	I(380)+I(396) / I(466)
PC (18:1/20:3)/(18:0/20:4)	I(404)+I(420)+I(466) / I(402)+I(418)
PE (18:1/18:1)/(18:2/18:0)	I(380)+I(396)+I(466) / I(464)
PE (18:0/18:2)/(18:2/18:0)	I(378)+I(394) / I(464)
PE (18:0/18:1)/(18:1/18:0)	I(380)+I(396) / I(466)
PC 16:0/16:1(*n*-9/*n*-7)	I(137)+I(226) / I(165)+I(254)
PC 16:1(*n*-9/*n*-7)/16:0	I(207)+I(296) / I(235)+I(324)
PC 16:1/18:1(*n*-9/*n*-7)	I(165)+I(254) / I(193)+I(282)
PC 18:1(*n*-9/*n*-7)/16:1	I(235)+I(324) / I(263)+I(352)
PC 16:0/18:1(*n*-9/*n*-7)	I(165)+I(254) / I(193)+I(282)
PC 18:1(*n*-9/*n*-7)/16:0	I(235)+I(324) / I(263)+I(352)
PC 18:1/18:1(*n*-9/*n*-7)	I(165)+I(254) / I(193)+I(282)
PC 18:1(*n*-9/*n*-7)/18:1	I(235)+I(324) / I(263)+I(352)
PC 18:0/18:1(*n*-9/*n*-7)	I(165)+I(254) / I(193)+I(282)
PC 18:1(*n*-9/*n*-7)/18:0	I(235)+I(324) / I(263)+I(352)

Supplementary Table 15. Lipids in single HepG2 cells identified by the tandem MS with miniature dual-LIT MS

No.	Name	Adduct	*m/z*	MS/MS Fragments
1	**PC 30:0**	M+H	706	184
2	**PC 31:1**	M+H	718	184
3	**PC 31:0**	M+H	720	184
4	**PC 32:2**	M+H	730	184
5	**PC 32:1**	M+H	732	184
6	**PC 32:0**	M+H	734	184
7	**PC 33:2**	M+H	744	184
8	**PC 33:1**	M+H	746	184
9	**PC 33:0**	M+H	748	184
10	**PC 34:3**	M+H	756	184
11	**PC 34:2**	M+H	758	184
12	**PC 34:1**	M+H	760	184
13	**PC 34:0**	M+H	762	184
14	**PC 35:2**	M+H	772	184
15	**PC 35:1**	M+H	774	184
16	**PC 35:0**	M+H	776	184
17	**PC 36:3**	M+H	784	184
18	**PC 36:2**	M+H	786	184
19	**PC 36:1**	M+H	788	184
20	**PC 36:0**	M+H	790	184
21	**PC 37:2**	M+H	800	184
22	**PC 38:6**	M+H	806	184
23	**PC 38:5**	M+H	808	184
24	**PC 38:4**	M+H	810	184
25	**PC 38:3**	M+H	812	184
26	**PC 38:2**	M+H	814	184
27	**PC 39:4**	M+H	824	184
28	**PC 39:3**	M+H	826	184

No.	Name	Adduct	*m/z*	MS/MS Fragments
29	**PC 40:5**	M+H	836	184
30	**PC 40:4**	M+H	838	184
31	**PC 40:3**	M+H	840	184
32	**PC 40:2**	M+H	842	184
33	**PE 34:1**	M+H	718	577
34	**PE 34:0**	M+H	720	579
35	**PE 35:2**	M+H	730	589
36	**PE 35:1**	M+H	732	591
37	**PE 36:2**	M+H	744	603
38	**PE 36:1**	M+H	746	605
39	**PE 36:0**	M+H	748	607
40	**PE 38:4**	M+H	768	627
41	**PE 38:2**	M+H	772	631
42	**PE 38:1**	M+H	774	633
43	**PE 40:6**	M+H	792	651
44	**PE 40:5**	M+H	794	653
45	**PE 40:2**	M+H	800	659
46	**PE 42:6**	M+H	820	679
47	**PE 42:4**	M+H	824	683
48	**PE 42:3**	M+H	826	685
49	**PS 36:3**	M+H	786	601
50	**PS 36:2**	M+H	788	603
51	**PS 38:6**	M+H	808	623
52	**PS 38:5**	M+H	810	625
53	**PS 38:4**	M+H	812	627
54	**PS 40:5**	M+H	838	653
55	**PS 40:4**	M+H	840	655
56	**SM 34:1**	M+H	703	184

Supplementary Table 16. Lipid isomers with C=C locations in single HepG2 cells identified by the tandem MS with miniature dual-LIT MS

No.	Name	Adduct	*m/z*	PB product	Diagnostic Ions	C=C location
1	PC 32:1	M+H	732	853	608, 697	**PC 16:0_16:1(n-10)**
2					622, 711	**PC 16:0_16:1(n-9)**
3					650, 739	**PC 16:0_16:1(n-7)**
4	PC 34:2	M+H	758	879	634, 723	**PC 16:1_18:1(n-10)**
5					648, 737	**PC 16:1_18:1(n-9)**
6					676, 765	**PC 16:1_18:1(n-7)**
7					650, 739; 690, 779	**PC 16:0_18:2(n-6, 9)**
8	PC 34:1	M+H	760	881	636, 725	**PC 16:0_18:1(n-10)**
9					650, 739	**PC 16:0_18:1(n-9)**
10					678, 767	**PC 16:0_18:1(n-7)**
11	PC 36:3	M+H	784	905	636, 725; 676, 765; 716, 805	**PC 16:0_20:3(n-6, 9, 12)**
12					674, 763; 676, 765; 716, 805	**PC 18:1(n-9)_18:2(n-6, 9)**
13					702, 791; 676, 765; 716, 805	**PC 18:1(n-7)_18:2(n-6, 9)**
14	PC 36:2	M+H	786	907	678,767;718,807	**PC 18:0_18:2(n-6,9)**
15					662, 751	**PC 18:1(n-10)_18:1(n-10)**
16					676, 765	**PC 18:1(n-9)_18:1(n-9)**
17					704, 793	**PC 18:1(n-7)_18:1(n-7)**
18	PC 36:1	M+H	788	909	664, 753	**PC 18:0_18:1(n-10)**
19					678, 767	**PC 18:0_18:1(n-9)**
20					706, 795	**PC 18:0_18:1(n-7)**
21	PC 38:5	M+H	808	929	698, 787; 620,709;660, 749; 700, 789; 740, 829	**PC 18:1(n-9)_20:4(n-6, 9, 12, 15)**
22					726, 815; 620,709; 660, 749; 700, 789; 740, 829	**PC 18:1(n-7)_20:4(n-6, 9, 12, 15)**
23					622, 711; 662, 751; 702, 791; 742, 831;782,871	**PC 18:0_20:5(n-3, 6, 9, 12, 15)**
24	PE 36:1	M+H	746	867	481, 570	**PE 18:0_18:1(n-10)**
25					495, 584	**PE 18:0_18:1(n-9)**
26					523, 612	**PE 18:0_18:1(n-7)**

Supplementary Table 17. Lipid isomers with *sn*-positions in single HepG2 cells identified by the tandem MS with miniature dual-LIT MS

No.	Name	Adduct	*m/z*	PB product	Diagnostic Ions	*sn*-position
1	PC 32:1	M+Na	754	875	352, 368	**PC16:0/16:1**
2					438	**PC16:1/16:0**
3	PC 34:2	M+Na	780	901	380, 396, 438	**PC 16:1/18:1**
4					352, 368, 466	**PC 18:1/16:1**
5					378, 394	**PC 16:0/18:2**
6					464	**PC 18:2/16:0**
7	PC 34:1	M+Na	782	903	380, 396	**PC 16:0/18:1**
8					466	**PC 18:1/16:0**
9	PC 36:3	M+Na	806	927	404, 420	**PC 16:0/20:3**
10					378, 394, 466	**PC 18:1/18:2**
11					380, 396, 464	**PC 18:2/18:1**
12	PC 36:2	M+Na	808	929	380, 396, 466	**PC 18:1/18:1**
13					378, 394	**PC 18:0/18:2**
14					464	**PC 18:2/18:0**
15	PC 36:1	M+Na	810	931	380, 396	**PC 18:0/18:1**
16					466	**PC 18:1/18:0**
17	PC 38:5	M+Na	830	951	402, 418, 466	**PC 18:1/20:4**
18					400, 416	**PC 18:0/20:5**
19	PE 36:1	M+Na	768	889	380, 396	**PE 18:0/18:1**
20					466	**PE 18:1/18:0**

References

[1] X. Ma, W. Zhang, Z. Li, Y. Xia, Z. Ouyang, *Acc. Chem. Res.* **2021**, *54*, 3873-3882.

[2] N. Li, X. Zhou, Z. Ouyang, *Int. J. Mass Spectrom.* **2021**, *462*.

[3] Z. Pang, J. Chong, G. Zhou, D. A. de Lima Morais, L. Chang, M. Barrette, C. Gauthier, P. E. Jacques, S. Li, J. Xia, *Nucleic Acids Res.* **2021**, *49*, W388-W396.

[4] X. Zhou, X. Liu, Z. Ouyang, *J. Am. Soc. Mass Spectrom.* **2020**, *31*, 429-433.

[5] B. Seashore-Ludlow, M. G. Rees, J. H. Cheah, M. Cokol, E. V. Price, M. E. Coletti, V. Jones, N. E. Bodycombe, C. K. Soule, J. Gould, B. Alexander, A. Li, P. Montgomery, M. J. Wawer, N. Kuru, J. D. Kotz, C. S. Hon, B. Munoz, T. Liefeld, V. Dancik, J. A. Bittker, M. Palmer, J. E. Bradner, A. F. Shamji, P. A. Clemons, S. L. Schreiber, *Cancer Discov.* **2015**, *5*, 1210-1223.